A flux tower site attribute dataset intended for land surface modeling

Jiahao Shi[1], Hua Yuan[1], Wanyi Lin[1], Wenzong Dong[1], Hongbin Liang[1], Zhuo Liu[1], Jianxin Zeng[1], Haolin Zhang[1], Nan Wei[1], Zhongwang Wei[1], Shupeng Zhang[1], Shaofeng Liu[1], Xingjie Lu[1], Yongjiu Dai[1]

[1]Southern Marine Science and Engineering Guangdong Laboratory (Zhuhai), Guangdong Province Key Laboratory for Climate Change and Natural Disaster Studies, School of Atmospheric Sciences, Sun Yat-Sen University, Zhuhai 519082, China

Correspondence to: Hua Yuan (yuanh25@mail.sysu.edu.cn)

Abstract. Land surface models (LSMs) require~~should have~~ reliable forcing, validation, and surface attribute data as the foundation for effective model development and improvement. Eddy covariance flux tower data are widely regarded as ~~considered~~ the benchmark~~ing data~~ for LSMs. However, currently available flux tower datasets often require multiple aspects of processing to ensure data quality before application to LSMs. More importantly, these datasets frequently lack site-observed attribute data, such as fractional vegetation cover and leaf area index, which limits their utility as benchmarking data.~~limiting their use as benchmarking data.~~ Here, we conducted a comprehensive quality screening of the existing reprocessed flux tower dataset, including the proportion of gap-filled data, energy balance closure (EBC), and external disturbances such as irrigation and deforestation,~~external disturbances, and energy balance closure (EBC),~~ leading to 90 high-quality sites. For these sites, we collected vegetation, soil, and topography ~~information~~data, ~~and~~ as well as wind speed, temperature, and humidity measurement heights from literature, regional networks, and Biological, Ancillary, Disturbance, and Metadata (BADM) files. We then compiled the final flux tower attribute dataset by filling in missing attributes with global data and classifying plant functional types (PFTs)~~Then we obtained the final flux tower attribute dataset by global data product complement and plant functional types (PFTs) classification~~. This dataset is provided in NetCDF format ~~complete~~ with necessary descriptions and reference sources. Model simulations revealed substantial disparities in output between the attribute data observed at the site and those commonly used by LSMs~~the defaults of the model~~, underscoring the critical role of site-observed attribute data and increasing the emphasis on flux tower attribute data in the LSM community. The dataset addresses the lack of site attribute ~~data~~ to some extent, reduces uncertainty in LSM~~s~~ data source, and aids in diagnosing parameter as well as process deficiencies. The dataset is available at https://doi.org/10.5281/zenodo.12596218~~https://doi.org/10.5281/zenodo.10939725~~ (Shi et al., 2024).

1 Introduction

Land surface models (LSMs) simulate the exchange of carbon, water and energy fluxes between soil, vegetation and atmosphere, and are essential tools for comprehending and predicting mass and energy interactions between the earth's biosphere and atmosphere (Pitman, 2003; Williams et al., 2009). The key role of LSMs is to provide the land surface boundary conditions for climate and weather forecast models (Mariotti et al., 2018; Pitman, 2003), as well as uncoupled stand-alone runs to investigate terrestrial water resources, ecology, and carbon storage (Crow et al., 2012; Humphrey et al., 2021; Ukkola et al., 2016a). Therefore, LSMs offer valuable insights for addressing environmental issues and mitigating climate change. Offline (i.e., uncoupled) LSMs are forced by meteorological data including wind speed, air temperature, specific humidity, air pressure, precipitation, and downward longwave and shortwave radiation. Flux towers measure the cycling of carbon, water and energy between the biosphere and atmosphere, providing observations with meteorological data that can be used to force offline LSMs. These observations are characterized by high temporal resolution (typically 30 min), continuous observations, direct flux measurements~~measure fluxes directly~~, and often ~~over~~ span multiple years. For these reasons, they are regarded as benchmarking data for LSMs calibration, evaluation, and enhancement, enabling model development~~allowing the development of models~~ from sub-daily to seasonal and interannual scales. Numerous studies have leveraged flux tower data for developing LSMs (Best et al., 2015; Blyth et al., 2010; Harper et al., 2021; Melton et al., 2020; Stevens et al., 2020; Ukkola et al., 2016b; Zhang et al., 2017; Stockli et al., 2008). However, despite their significance, flux tower data were ~~was~~ not originally designed for testing and validating LSMs. When applied to LSMs, these datasets suffer from poor data quality and a deficiency of site attribute data.~~it suffers from poor data quality and a deficiency of attribute data.~~

FLUXNET2015 is currently the most widely used flux tower dataset (Pastorello et al., 2020) . However~~, but~~ substantial preprocessing is frequently required to ensure the reliability of meteorological forcing and flux assessment data for LSM ~~applications~~. To reduce ~~the~~ repetitious data processing efforts and improve consistency, Ukkola et al. (2022) integrated three flux tower datasets (FLUXNET2015, La Thuile, and OzFlux)~~,~~ and then performed screening, gap-filling, and other procedures to resolve issues such as missing data and energy balance closure (EBC)~~ within these datasets~~. This effort resulted in~~As a result,~~ a dataset called PLUMBER2, comprising~~with a total of~~ 170 high-quality sites is tailored for LSMs. This work considered as many available flux tower datasets as possible and used an automated, reproducible data screening process. However, ~~It's worth noting, though, that~~ the PLUMBER2 dataset only performs quality checks on meteorological forcing data, ~~and~~ not on flux assessment data, to obtain more available years of data and enable models to be assessed against specific weather and climate events. Consequently, a large proportion of gap-filled flux data is present ~~in~~ at some sites. Land surface modelers typically employ~~usually go through~~ stringent quality control procedures to avoid misleading model evaluation results (Blyth et al., 2010; Li et al., 2019; Purdy et al., 2016). Therefore~~Thus~~, these existing gap-filled data still require further processing.

Most importantly, these flux tower datasets lack site-observed vegetation, soil, and topography ~~information~~ data such as fractional vegetation cover (FVC), Leaf Area Index (LAI), soil texture, slope and aspect. For regional and single-point modeling, the current practice ~~involves deriving~~usually involves obtaining these attribute data for LSMs through the inversion of global satellite observations. This approach introduces additional~~raises the~~ uncertainty ~~of~~ into LSMs and diminishes the utility ~~usefulness~~ of flux tower data as benchmarking data for ~~evaluating the~~ model evaluation.

Uncertainty in vegetation and soil data constitutes a significant source of uncertainty in LSMs (Dai et al., 2019b; Li et al., 2018). Vegetation composition and density play a prominent role ~~part~~ in modulating the surface energy budget (Bagley et al., 2017; Williams and Torn, 2015), by altering canopy conductance, aerodynamic properties, and albedo, ultimately affecting water and energy fluxes between the surface and atmosphere (Anderson et al., 2011; Bonan, 2008). Similarly, soil texture directly influences ~~affects~~ various soil hydrological and thermodynamic parameters, including saturated soil water content and soil thermal conductivity (Arya and Paris, 1981; Minasny and McBratney, 2007). These parameters~~, which~~ have a substantial ~~great~~ impact on soil temperature and moisture, as well as ~~and~~ the terrestrial carbon and water cycle (Dirmeyer, 2011; Entekhabi et al., 1996). Although recent LSM development has attempted to use site-observed attribute data to reduce uncertainty in model results (Harper et al., 2021; Melton et al., 2020), the data used in these studies are typically limited and not publicly available, making it challenging for other researchers to apply these valuable data. Generally speaking, no flux tower dataset can be used directly in developing ~~the building of~~ LSMs, and they frequently lack the necessary site-observed information about soil, vegetation, and other attributes.

To provide more accurate and reliable flux tower data for LSM~~s~~ modeling and validation~~, in this study~~, we conducted thorough quality control for the site data based on the PLUMBER2 dataset produced by Ukkola et al. (2022), resulting in a total of 90 sites. Subsequently, we carried out an extensive collection of available flux tower attribute data~~ is carried out~~, drawing from sources such as site-related literature and websites. We~~The attribute data is~~ further complemented the attribute data with ~~by~~ global data~~ products~~. As a result~~In the end~~, we generated a flux tower dataset that can be directly applied to LSMs and contains essential attribute data. Furthermore, through modeling comparison for the four key attribute variables—percentage of plant functional type (PFT) cover (PCT_PFT), LAI, canopy height, and soil texture—we demonstrate how the outputs differ between site-observed attributes and the default attribute data employed by an LSM. These results emphasize the non-negligible impact of flux tower attribute data on model simulation and development.~~Furthermore, by modeling for the four most important attribute variables – percentage of plant functional type (PFT) cover (PCT_PFT), LAI, canopy height and soil texture – we demonstrate how the site-observed attribute data and the conventional attribute data used by LSMs differ in their model output. These results emphasize the non-negligible impact of flux tower attribute data in model simulation and its development.~~

2 Data and Methods

2.1 Datasets

The data used in this study can be categorized into four groups~~groupings~~, as~~ Table 1~~ illustrated~~s~~ in Table 1. Firstly, PLUMBER2 serves as the dataset for data quality screening. The second group comprises~~is ~~the attribute sources, including 113 site-related literature, seven ~~7 ~~flux regional networks, and the Biological, Ancillary, Disturbance, and Metadata (BADM) files provided by FLUXNET and AmeriFlux.

The third category includes data sources employed for PFTs classification, incorporating 7 site-related articles for C3/C4 classification, flux tower site measurements of precipitation and air temperature, global maps of the Köppen-Geiger climate classification, and the reprocessed MODIS Version 6.1 Leaf Area Index dataset. The Köppen-Geiger climate classification maps, presented at ~~an unprecedented ~~1 km resolution, are derived from an ensemble of four high-resolution, topographically corrected climatic maps. They demonstrate higher classification accuracy and substantially more detail than previous versions. The reprocessed MODIS LAI used the modified temporal spatial filter (mTSF) method for simple data assimilation, then applied the post processing-TIMESAT (a software package to analyze time-series of satellite sensor data) Savitzky–Golay (SG) filter to obtain the result. Site LAI validation shows that the reprocessed MODIS LAI is much smoother and more consistent with adjacent values than the original MODIS LAI, and closer to site observations (Lin et al., 2023; Yuan et al., 2011).~~And the reprocessed MODIS LAI is much smoother and more consistent with adjacent values, displaying better spatiotemporally continuous and consistency.~~

Finally, three global datasets were used to fill in ~~complement ~~attribute data of sites lacking site-observed FVC, LAI, and soil texture. LAI filling still uses the reprocessed MODIS LAI, whereas the FVC filling employs a global 300 m PFT map~~LAI complements still use the reprocessed MODIS LAI. FVC complements use a global 300m PFT map~~, PFT_{local} (Harper et al., 2023). PFT_{local} incorporates a variety of currently available high-resolution satellite data to quantify the percentage of PFT in each 300 m pixel worldwide. The 300m resolution is well-matched with the regional extent of the flux tower footprint (Chu et al., 2021), providing representative FVC data. ~~Complements ~~Filling of soil texture ~~using ~~uses the Global Soil Dataset for Earth System Models (GSDE) (Shangguan et al., 2014). The GSDE harmonizes ~~the~~ data collected from various sources and uses a standardized data structure and data processing procedures to derive the final dataset. It has been~~is ~~extensively applied in e~~E~~arth system models (Dai et al., 2019a).

2.2 Processing Methods

We undertook three primary ~~processing ~~steps to establish the final dataset: site and time period selection, attribute collection, and data processing. First~~ly~~, the data selection process involves picking years with a low gap-filled percentage for fluxes (latent and sensible heat) and vapor pressure deficit (VPD), ~~while ~~excluding sites subject to external disturbances ~~and ~~or unable to undergo~~go through~~ EBC checks. Following that, we collected site-observed vegetation, soil, and topography data. ~~The ~~V~~v~~egetation attributes includ~~ed~~ FVC, maximum LAI and mean canopy height. ~~The s~~Soil attributes includ~~ed~~ soil texture, bulk density, organic carbon concentration and depth~~bulk density and organic carbon concentration~~. ~~The~~ ~~T~~Ttopography attributes includ~~ed~~ ~~elevation,~~ slope and aspect. Additionally~~Besides~~, we obtained the reference measurement heights (for emulating the lowest layer of the atmospheric model to which the LSM would be coupled) of wind speed, air temperature and humidity.~~the reference measurement height (for emulating the lowest layer of the atmospheric model to which the LSM would be coupled) was revised by wind speed measurement height if possible.~~ Then, we filled in ~~complemented~~ t FVC, maximum LAI,~~he vegetation attributes~~ and soil texture using global datasets~~data~~. Finally, the FVC was further ~~breakdown to~~broken down into different PFTs. Figure 1 presents a flowchart of the processing pipeline, with each step described in detail below.

Table 1. Summary of the data sources to derive the site attribute dataset.

Data usage	**Name**	**Sources**
For s~~S~~ite and time period selection	PLUMBER2	Ukkola et al., 2022
Attribute data	Site descriptions in literature (113 articles)	Details in Table S1
	Site regional networks (7 websites)	AmeriFlux[a]; AT – Neu websit[a]; ChinaFlux[c]; European Fluxes[d] Global Monitoring Labortatory[e]; OzFlux[f]; Swiss Fluxnet[g]
	Fluxnet BADM	https://fluxnet.org/
	AmeriFlux BADM	https://ameriflux.lbl.gov/
PFT information	Site descriptions in literature (7 articles)	Details in Table S1
	Site measurements of precipitation and air temperature	Ukkola et al., 2022
	Köppen-Geiger climate classification maps	Beck et al., 2018
	Reprocessed MODIS Version 6.1 LAI dataset	Lin et al., 2023
Data ~~complement~~filling	PFT_{local} PFTs maps	Harper et al., 2023
	Reprocessed MODIS Version 6.1 LAI dataset	Lin et al., 2023
	Global soil dataset for earth system models	Shangguan et al., 2014

[a] https://ameriflux.lbl.gov/, [b] http://www.biomet.co.at/, [c] http://www.chinaflux.org/, [d] http://www.europe-fluxdata.eu/, [e] https://www.gml.noaa.gov/, [f] https://ozflux.org.au/, [g] https://www.swissfluxnet.ethz.ch/.

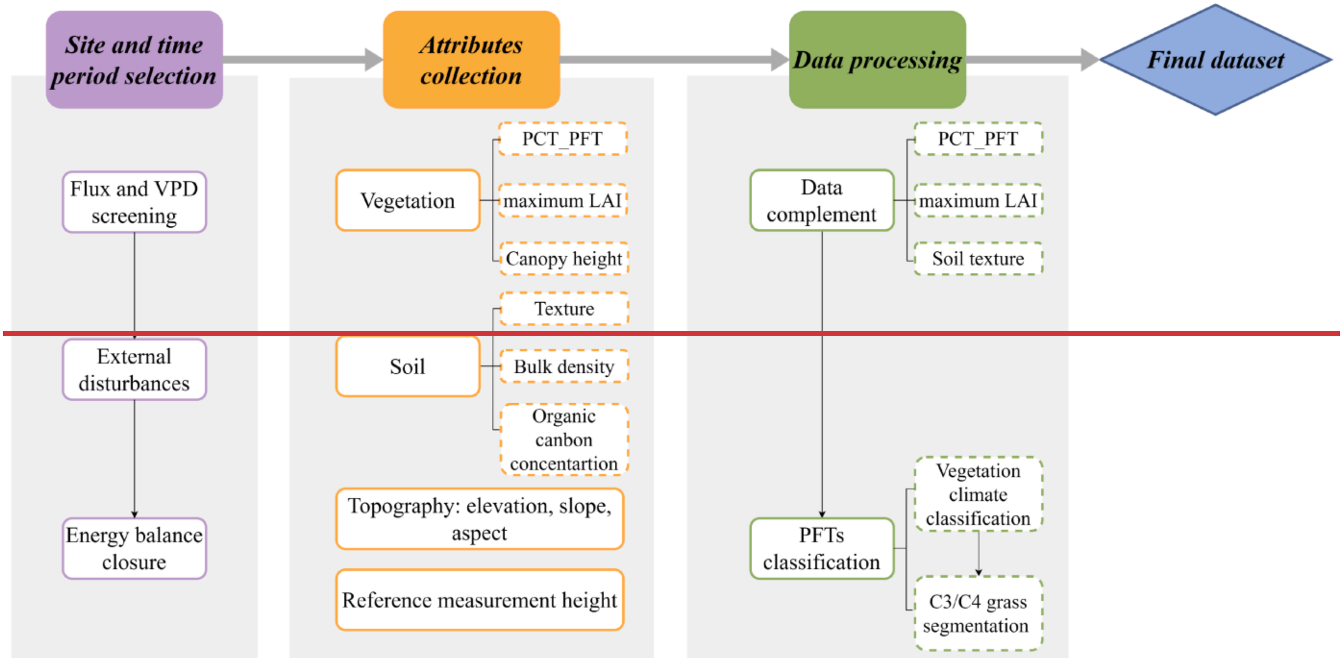

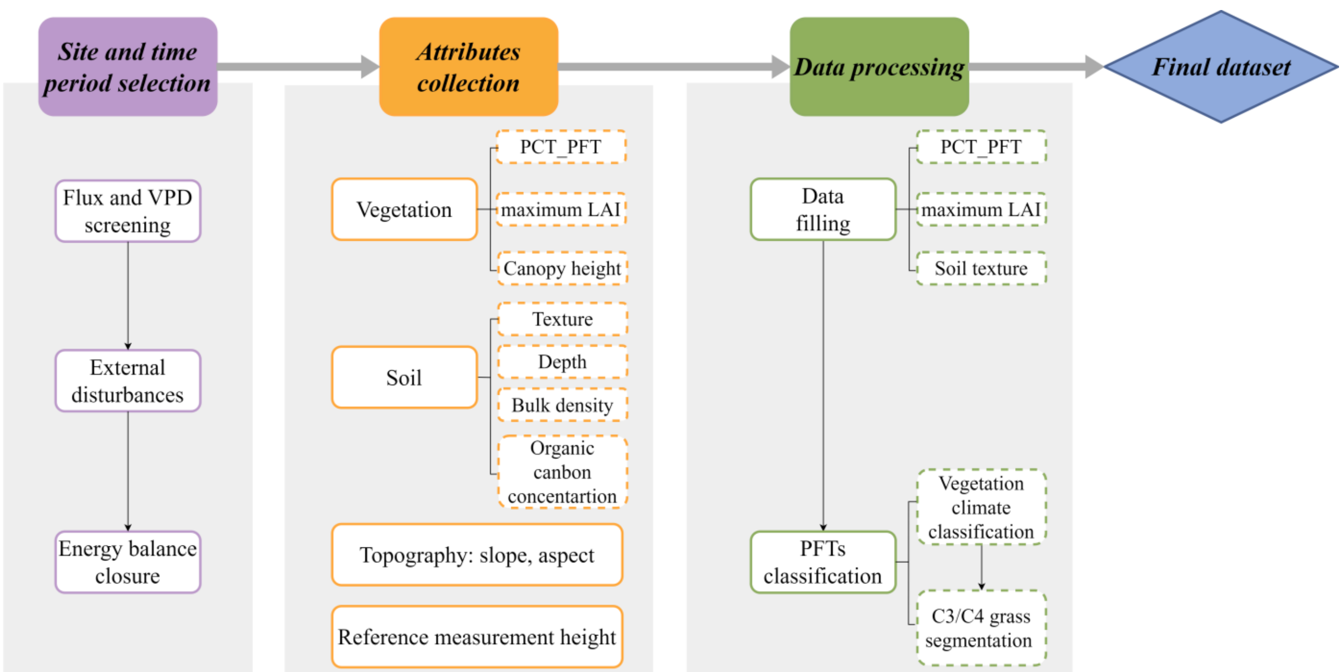

Figure 1. Data flow diagram for the generation of the flux tower attribute dataset.

2.2.1 Site and time period selection

The PLUMBER2 dataset got 170 sites by screening meteorological data (including five key variables that have the largest influence on LSM simulations: incoming shortwave radiation, precipitation, air temperature, air humidity, and wind speed.).~~The PLUMBER2 dataset got 170 sites by screening meteorological data.~~ For FLUXNET2015 and La Thuile datasets, specific humidity is not provided in the original data, so it was calculated from VPD (Ukkola et al., 2017). However, the screening process did not consider~~take into account~~ the gap-filled situation of VPD. As mentioned earlier, it also did not screen the flux variables. To address these limitations, we further implemented quality control on the PLUMBER2 dataset by performing the following three steps:

1. Sites with only one year of observations were excluded to ensure data stability and reliability.
2. Selected the years where the proportion of data with fluxes (latent and sensible heat) quality control (QC) ≤ 1 exceeds 90 % (QC = 0 denotes observed data, QC = 1 represents high-quality gap-filled data in FLUXNET2015 and La Thuile, no QC = 1 in OzFlux).
3. Selected the years where the proportion of VPD QC = 0 exceeds 90 % in FLUXNET2015 and La Thuile datasets.

Furthermore, we excluded 23 sites that lacked ground heat flux observations because the EBC correction factor (f_{EBC}) could not be calculated (f_{EBC} = (Rn - G) / (~~LE~~ Qle + Qh~~H~~), net radiation (Rn), ground heat flux (G), latent heat flux (~~LE~~Qle) and sensible heat flux (Qh~~H~~)). Additionally, two sites (FR-Lq1 and FR-Lq2) were removed as they have a very low energy closure rat~~d~~io (EBR, calculated as (~~LE~~ Qle + Qh~~H~~) / (Rn – G) according to Wilson et al. (2002)) after performing energy closure (~~sites FR-Lq1 and FR-Lq2,~~ details~~ed~~ in Table S3). Lastly, we excluded 10 sites that experienced external disturbances during the observation period, such as irrigation, deforestation, and one site impacted by a ~~sizable~~ large ~~body of~~ water body nearby (details in Table S3). In the end, we preserved non-consecutive years that met ~~the~~ our criteria. This allows us to maximize the utility of valuable observational data. Details of the selected and excluded sites and years are displayed in Tables S2 and S3.

2.2.2 Data collection for vegetation attributes

Percent cover of plant functional types

~~Percent plant functional types cover~~

FVC data was ~~is~~ sourced from site descriptions in literature, regional networks, and FLUXNET BADM files. We sought ~~looked for~~ appropriate representations of site FVC and obtained site-observed FVC ~~information~~ data for ~~at~~ 53 sites. To maximize the amount of FVC collected, some assumptions were made~~We made assumptions~~ ~~in~~ at certain sites during the data collection process~~FVC collection to get as much FVC data as possible~~, addressing scenarios as follows:

1. For sites lacking explicit FVC data but providing the percentage of vegetation flux footprint contribution or dense forest canopy basal area~~For sites lacking a direct FVC representation but providing information on the percentage~~

~~of vegetation flux footprint contribution or dense forest canopy basal area~~, we treated these values~~also treat them~~ as FVC. ~~Because~~ Since FVC directly determines these metrics~~this information~~, and they are ~~close~~ numerically similar.

2. In grassland and cropland sites, the vegetation cover type typically exhibits a high degree of homogeneity.~~In the case of grassland and cropland sites, both surface cover landscapes are usually homogeneous cover and manual management.~~ Therefore, we referred to site pictures (photographs taken at the site) to make a judgment~~we referred to site pictures to make a judgment~~. If a homogeneous cover could be determined from the pictures, it was assigned a 100 % coverage percentage.
3. Some grassland sites with annual vegetation ~~There~~ may experience ~~be~~ seasonal bare soil exposure~~in some grassland sites with annual vegetation~~. For these sites, we used the FVC during the peak vegetation growth period.
4. In forest sites, we simply ~~We~~ treated forest litter as ~~if it were~~ grass cover in the absence of additional information~~since bare soil may not be present in forests~~.

After that, trees and shrubs were classified as evergreen or deciduous, coniferous or broadleaf, based on their vegetation type. As an example, eucalyptus trees are classified as evergreen broadleaf trees. For data completeness, we used the PFT_{local} maps to fill in data for sites lacking site-observed FVC values.

We further broke down the FVC into PFTs to meet the requirements of LSM simulations using PFTs. The breakdown method is as follows: First, the climate type of PFT was determined according to the Köppen climate classification (Poulter et al., 2011). Then, C3 and C4 grasses were partitioned using site descriptions. If site descriptions were unavailable, flux tower air temperature, precipitation, and the reprocessed MODIS LAI are used to calculate LAI proportions under C3/C4 climatic conditions, thereby estimating the C3/C4 grass proportions (Still et al., 2003).

~~For data completeness, we used the PFT_{local} maps to complement the data for sites lacking site-observed vegetation cover proportion. After that, we further breakdown the FVC data in terms of different PFTs to align with the requirements of LSMs simulation using PFTs. First, trees and shrubs were classified as evergreen or deciduous, as well as coniferous or broadleaf types, based on the vegetation type expressed in the data sources. Next, Köppen-Geiger climate classification maps are employed to categorize the climate type of PFTs using the method proposed by Poulter et al. (2011). To better represent the C3 and C4 grasses, we prioritize segmentation based on the data source descriptions. If site description was not available, then segmentation was performed using the Still et al. (2003) method, which uses flux tower air temperature, precipitation, and reprocessed MODIS Version 6.1 LAI.~~

A total of 16 PFTs includes the original ~~full~~ set of 15 PFTs initially developed by Bonan et al. (2002) supplemented with a new bare soil surface type. The full set of PFTs includes bare soil; Needleleaf evergreen tree, temperate (ENT_Te); Needleleaf evergreen tree, boreal (ENT_Bo); Needleleaf deciduous tree (DNT); Broadleaf evergreen tree, tropical (EBT_Tr); Broadleaf evergreen tree, temperate (EBT_Te); Broadleaf deciduous tree, tropical (DBT_Tr); Broadleaf deciduous tree, temperate (DBT_Te); Broadleaf deciduous tree, boreal (DBT_Bo); Broadleaf evergreen shrub, temperate (EBS_Te); Broadleaf deciduous shrub, temperate (DBS_Te); Broadleaf deciduous shrub, boreal (DBS_Bo); C3 grass, arctic; C3 grass; C4 grass; Crop. This PFTs classification scheme is widely utilized in LSMs.

Maximum leaf area index

Maximum LAI data were primarily ~~is~~ sourced from site descriptions in literature and AmeriFlux BADM files which could be~~.~~ ~~Included are~~ the explicitly stated maximum LAI values or those derived~~and the maximum LAI acquired~~ from interannual scatterplots. To maximize data availability~~Similarly~~, we made the following assumptions ~~in~~ at certain sites ~~to get as much data as possible~~. Specifically, ~~the~~ summertime LAI observation was considered~~is used~~ as the maximum LAI. And ~~we accept LAI to be maximum~~ when a single ~~the~~ LAI value was provided ~~for a single site is provided~~ without observation time or ~~additional~~ supporting information, it was accepted as the maximum LAI. To ensure data transparency, quality control flags were implemented~~. To distinguish such instances, we have positioned quality control flags~~ in the final dataset, allowing users~~.~~ ~~Users are free~~ to select data based on their acceptance criteria~~how accepting they are~~. A total of 67 site observations of maximum LAI were collected, with 33 ~~of these~~ sites providing ~~information on~~ the year of observation. For data completeness, we used the reprocessed MODIS Version 6.1 LAI dataset to ~~complement~~ fill in missing site-observed maximum LAI data~~the data for sites in case of site-observed maximum LAI was unavailable~~.

Canopy height

We calculated the mean canopy height over the observation period for 69 sites included in FLUXNET2015 dataset, using the canopy heights reported in FLUXNET BADM file across different periods. The mean canopy height provides a more truthful representation of the vegetation condition during the period of observation. For the remaining 21 sites, the canopy height provided by PLUMBER2 was used.

2.2.3 Data collection for soil attributes

Soil texture

Soil texture data ~~is~~ were sourced from site descriptions in literature, regional networks, and AmeriFlux BADM files. These descriptions provided information in two forms:~~encompass both~~ ~~: explicitly stated the~~ percentages of sand, silt, and clay, and (2) soil texture types ~~and the different types of soil textures~~, such as sandy loam. For the ~~The~~ latter, which do~~es~~ not ~~directly~~ provide ~~give~~ the percentages of sand, silt, and clay. So, we referred to the soil composition table presented ~~shown~~ by Dy and Fung (2016) to derive the~~, enabling the derivation of~~ specific proportions. This ~~The~~ table classifies soil into 16 categories based on the proportions of sand, silt, and clay. Overall~~In total~~, 72 site observations of soil texture were collected, with 34 sites providing ~~supplying~~ information on the depth of observations. For data completeness, we used the GSDE dataset to ~~complement~~ fill in the data for sites lacking site-observed soil texture.

Soil bulk density, organic carbon concentration, and depth

Soil bulk density, organic carbon concentration, and depth data were sourced from site descriptions in literature, regional networks, and AmeriFlux BADM file. Specifically, soil bulk density was collected at 37 sites, soil organic carbon concentration at 23 sites, and soil depth at 31 sites. The observation depth was recorded for soil bulk density at 32 sites and for organic carbon concentration at 22 sites. Despite the limited availability of site-observed data for the three soil attributes, we included them in the final dataset. For researchers conducting site-specific studies, these data can serve as valuable references.

~~**Soil bulk density and organic carbon concentration**~~

~~Soil bulk density and organic carbon concentration data are sourced from site descriptions in literature, regional networks, and AmeriFlux BADM file. Specifically, soil bulk density data were collected at 37 sites, and soil organic carbon concentration at 23 sites. At 32 and 22 sites, respectively, the observation depth was given. Despite the scarcity of site-observed data for these two soil attributes, we have included them in the final dataset. For site-specific studies, they can provide useful references for researchers.~~

2.2.4 Data collection for topography attributes

The topography data encompasses site ~~elevation,~~ slope and aspect. These data were ~~are~~ gathered from site descriptions in literature, regional networks, FLUXNET and AmeriFlux BADM files. Specifically, we acquired ~~elevation for 89 sites,~~ slope for 57 sites, and aspect for 49 sites from these ~~reference~~ sources. ~~In the AU-Lit site, where site elevation data was unavailable from the aforementioned references, we used the elevation given in Ukkola et al. (2022).~~

2.2.5 Reference measurement height

Site descriptions in literature, regional networks, FLUXNET and AmeriFlux BADM files were ~~are~~ all sources ~~of~~ for the reference measurement heights. From these sources,~~.~~ we searched ~~look~~ for the heights of wind speed, air temperature, and air humidity measurements or the height of the instrument used for these measurements (e.g., wind cups and temperature and humidity sensors).~~wind speed measurement or the height of instrument used to wind speed measurements (such as the wind cup).~~ In cases ~~instances~~ where the flux tower meteorological observation equipment lacked a dedicated wind speed measurement device~~lacks an individual wind speed observation apparatus~~, we assumed ~~suppose~~ that the use of three-dimensional sonic anemometer for wind speed measurements. Consequently~~As a result~~, wind observation heights were ~~are~~ available for a total of 76 sites, while 65 sites had temperature and humidity observation heights.~~.~~ For the remaining ~~14~~ sites where ~~wind~~ observation heights were not reported, we used the flux observation height as a substitute.

2.3 Modeling assessment of attribute data

The impact of collected attributes on carbon, water, and energy fluxes is assessed through single-point simulations using the latest version of the Common Land Model (Dai et al., 2003) (CoLM202X, https://github.com/CoLM-SYSU/CoLM202X/tree/master, last access: 21 November 2023). CoLM202X incorporates processes related to biogeophysics, biogeochemistry, ecological dynamics and human activities, and offers optional processes and schemes which can be customized by the user. In our experiments, vegetation is modeled using a set of time-invariant parameters (optical properties: leaf optical properties; morphological properties: canopy height, vegetation root depth and profile, leaf size and angle distributions; and physiological properties). The dynamic vegetation module is turned off and the time-variant

LAI and stem area index (SAI) values are prescribed from the reprocessed MODIS LAI data (Lin et al., 2023; Yuan et al., 2011). The two-big-leaf model (Dai et al., 2004) is employed to calculate processes such as radiative transfer (Yuan et al., 2017), photosynthesis (Collatz et al., 1992; Farquhar et al., 1980), and stomatal conductance (Ball et al., 1987). Surface turbulent exchange is simulated using similarity theory (Brutsaert, 1982; Zeng and Dickinson, 1998). Total evapotranspiration includes evaporation from stems, leaves, and the ground, as well as vegetation transpiration. Surface and subsurface runoff consider factors such as terrain, groundwater level, precipitation, and infiltration rate. Additionally, the model accounts for processes including precipitation phase and intensity, canopy interception, vertical movement of water in snow and soil, and snow compaction (Dai et al., 2003).~~The impact of collected attributes on carbon, water, and energy fluxes is assessed through single-point simulations using the Common Land Model (CoLM) (Dai et al., 2003). We used its latest version, CoLM202X (https://github.com/CoLM-SYSU/CoLM202X/tree/master, last access: 21 November 2023).~~

~~Here, t~~The simulations aim to evaluate the differences ~~discrepancies~~ in model results between runs using site-observed attributes~~attributes observed at the site~~ and those commonly utilized by LSMs. For simplicity, we refer to site-observed data as "site data" and data commonly utilized by LSMs as "default data" in subsequent descriptions. We focus on ~~the~~ four crucial~~most essential~~ attributes, PCT_PFT, LAI, canopy height and soil texture, to demonstrate their corresponding impacts. In site data simulations, we scaled the default LAI time series to match the maximum LAI observed, corrected the default canopy height using site canopy height, and replaced the default topsoil texture (0-28.9 cm) with the site-observed soil texture. For sites with multiple PFTs, we calculated the LAI for each PFT using growing degree days and PCT_PFT values (Lawrence and Chase, 2007). Canopy height was divided into three categories based on PFTs (trees, shrubs, or grassland), using site data to adjust the default values for the corresponding group, while the other two groups retained their default values.

The default data generally rely on global LAI and soil texture mapping products, lookup table canopy height, and site IGBP (International Geosphere–Biosphere Programme) classifications to characterize surface vegetation and soil conditions. In this study, the default LAI and soil texture refer to the reprocessed MODIS version 6.1 LAI and the GSDE soil texture ~~as~~ shown in Table 1. Lookup table canopy heights are sourced from CoLM, while site IGBP classifications are obtained from FLUXNET and OzFlux. We selected ~~chose~~ ten sites for each ~~of the~~ attribute~~s~~—LAI, canopy height, and soil texture—where site data differ ~~the~~ most from default data (In the lookup table canopy height simulations, sites with zero plane displacement exceeding reference measurement height are excluded~~.~~). For the PCT_PFT analyses, sites with IGBP types that include combinations of trees and grasses~~sites with IGBP types that are a combination of trees and grasses~~ (OSH, WSA, SAV) were chosen, resulting in six available sites. Table 2 provides an overview of the selected sites along with their corresponding attribute information. Each site was simulated under three conditions: 1) using site data for all attributes at each site, 2) using default data for all attributes at each site, and 3) using default data for the corresponding attribute at sites selected for each attribute separately, while maintaining site data for the remaining attributes. The comparison between simulations (1) and (3) aims to demonstrate the individual impact of each attribute, while the comparison between simulations (1) and (2) shows the combined impact of all four attributes.~~These sites were simulated to show the respective impact of different attributes in model results. Table 2 provides an overview of the chosen sites along with their corresponding attribute information.~~

At each site, we ran ~~run~~ CoLM at either the half-hourly or hourly time resolution, depending on the forcing data provided ~~data available~~, for all years in the original dataset. Subsequent analyses were ~~are~~ conducted ~~exclusively~~ only for the years we ~~have~~ selected~~chosen~~. To reach an equilibrium in soil moisture and temperature, CoLM loops the atmospheric forcing data for each site's observation period until it reaches 50 years long.~~the first year of atmospheric forcing data was cycled. CoLM was recursively run at each site using a 20-year spin-up.~~ The discrepancy between site data and default data is compared by variables related to land surface energy, water, and photosynthesis processes,~~The discrepancy of site data relative to default data is compared by an ensemble of climate-related variables,~~ including latent heat (~~LE~~Qle), sensible heat (Qh~~H~~), net radiation (Rn), upward shortwave radiation (SWup), gross primary production (GPP), friction velocity (Ustar), surface~~(0-4.5cm)~~ soil water content~~-~~ (0-4.5cm) (SWC), and total runoff (TR).

To quantify the differences between the output from ~~the~~ site data and default data~~,~~ while accounting for seasonal fluctuations in the impacts of soil and vegetation on climate-related variables~~and considering the seasonal fluctuations in the impacts of soil and vegetation on climate-related variables~~ (Dirmeyer, 2011; Forzieri et al., 2020).~~,~~ ~~We~~we designed a statistical indicator called the percentage of mean difference (MD %) (Eq. 1).~~,~~ ~~which~~This indicator is calculated by expressing the mean difference for each month~~as the mean difference in each month expressed~~ as a percentage of the observed or default modeled annual mean~~mean for the year~~. We used m~~M~~ulti-year average time series ~~are used here~~ to capture more stable differences in output. In addition, we used delta root mean squared error (ΔRMSE) (Eq. 3) and Δ|Bias| (Eq. 5) to measure the differences in RMSE and Bias of the output between site and default data, allowing ~~enabling~~ us to assess the model's performance after incorporating ~~using~~ site data.

$$MD\,\% = \begin{cases} \dfrac{\left|\frac{1}{n}\sum_{i=1}^{n}\left(Mod_{site,i} - Mod_{default,i}\right)\right|}{\frac{1}{365}\sum_{j=1}^{365} Obs_j}, & for\ Qle\cancel{LE}, Qh\cancel{H}, Rn, SWup, GPP, and\ Ustar \\ \dfrac{\left|\frac{1}{n}\sum_{i=1}^{n}\left(Mod_{site,i} - Mod_{default,i}\right)\right|}{\frac{1}{365}\sum_{j=1}^{365} Mod_{default,j}}, & for\ SWC\ and\ TR \end{cases} \quad n = days\ of\ month \tag{1}$$

$$RMSE = \sqrt{\frac{\sum_i^n (Mod_i - Obs_i)^2}{n}} \tag{2}$$

$$\Delta RMSE = RMSE_{site} - RMSE_{default} \tag{3}$$

$$Bias = \frac{\sum_i^n ((Mod_i - Obs_i)}{n} \tag{4}$$

$$\Delta|Bias| = |Bias_{site}| - |Bias_{default}| \tag{5}$$

Where $Mod_{site,i}$ and $Mod_{default,i}$ are the predicted value using site data and default data, respectively. Obs_j is observed value. n is the number of paired values. $RMSE_{site}$ and $RMSE_{default}$ are the RMSE of the simulation results using site data and default data, respectively. $Bias_{site}$ and $Bias_{default}$ also correspond to the Bias in these results.

Table 2. Selected sites and their attribute values used in the modeling assessment for attribute data. The suffix "default" denotes ~~is for model~~ default data, and the "site" represents site data.

Site_LAI	Lat	Lon	LAI_max_default[a] (m^2/m^2)	LAI_max_site[b] (m2/m2)
DE-Bay	54.14	11.86	3.6	6.5
DE-Gri	50.94	13.51	6.5 (2004[c])	4.4 (2004)
DK-Lva	55.68	12.08	3.1 (2004)	6.9 (2004)
DE-Seh	58.87	6.44	3.2 (2009)	5.9 (2009)
IT-Cpz	41.70	12.37	5.4	3.5
US-GLE	41.36	-106.24	1.5	3.8
US-Goo	34.25	-89.87	4.5	2.0
US-KS2	28.60	-80.67	6.6 (2005)	2.7 (2005)
US-MMS	39.32	-86.41	7.0	5.2
US-MOz	38.74	-92.20	6.1 (2006)	4.0 (2006)
Site_TEX	**Lat**	**Lon**	**TEX-default[d]**	**TEX_site[b]**
AU-Cpr	-34.00	140.58	64/18/18	94/4/2
AU-DaP	-14.06	131.31	63/18/19	92/5/3
AU-DaS	-14.15	131.38	63/12/25	92/5/3
CZ-wet	49.02	14.77	39/37/32	10/85/5
DE-Gri	50.94	13.51	52/29/20	10/81/9 (0-23cm)
ES-LMa	39.94	-5.77	49/24/24	80/11/9 (0-30cm)
FI-Sod	67.36	26.63	52/25/20	92/5/3
IT-Cpz	41.70	12.37	33/45/22	87/8/5 (0-10cm)
IT-SRo	43.72	10.28	69/17/15	95/4/1 (10-20cm)
SD-Dem	13.28	30.47	67/18/14	96/4/0
Site_HTOP	**Lat**	**Lon**	**H_{can}_default[e] (m)**	**H_{can}_site[b] (m)**
AU-Lit	-13.17	130.79	35	20.0
BE-Vie	50.30	5.99	17	33.7
CH-Dav	46.81	9.85	17	25
DE-Hai	51.07	10.45	20	33.9
DE-Tha	50.93	13.56	17	28.4
IT-Cpz	41.70	12.37	35	14.3
IT-Lav	45.95	11.28	17	28.0
IT-Ren	46.58	11.43	17	29.0
RU-Fyo	56.46	32.92	17	26.3
US-Ton	38.43	-120.96	20	9.9
Site_FVC	**Lat**	**Lon**	**IGBP**	**PCT_PFT_site[b]**
AU-How	-12.49	131.14	WSA	EBT_Tr/DBS_Te/C4 : 50/25/25

ES-LMa	39.94	-5.77	SAV	EBT_Te/C3 : 20/80
SD-Dem	13.28	30.47	SAV	EBT_Tr/C3/C4 : 10/27/63
US-SRM	31.82	-110.86	WSA	DBS_Te/C3/C4 : 35/43/22
US-Ton	38.43	-120.96	WSA	EBT_Te/C3 : 40/60
US-Whs	31.74	-110.05	OSH	Bare/DBS_Te/C3 : 39/51/10

~~Site~~	~~LAI_default[a]~~	~~LAI_site[b] (m^2/m^2)~~	~~S~~	~~TEX_default[c]~~	~~TEX_site[b]~~
~~US-KS2~~	~~6.6 (2005[e])~~	~~2.7 (2005)~~	~~I~~	~~33/45/22~~	~~87/8/5~~
~~DK-Lva~~	~~3.1 (2004)~~	~~6.9~~	~~D~~	~~52/29/20~~	~~10/81/9~~
~~DE-Bay~~	~~3.6~~	~~6.5~~	~~F~~	~~52/25/20~~	~~92/5/3~~
~~US-Goo~~	~~4.5~~	~~2.0~~	~~E~~	~~49/24/24~~	~~80/11/9~~
~~DE-Seh~~	~~3.2 (2009)~~	~~5.9 (2009)~~	~~A~~	~~64/18/18~~	~~94/4/2~~
~~US-GLE~~	~~1.5~~	~~3.8~~	~~S~~	~~67/18/14~~	~~96/4/0~~
~~US-Moz~~	~~6.1 (2006)~~	~~4.0 (2006)~~	~~C~~	~~39/37/32~~	~~10/85/5~~
~~DE-Gri~~	~~6.5 (2004)~~	~~4.4 (2004)~~	~~A~~	~~63/18/19~~	~~92/5/3~~
~~IT-Cpz~~	~~5.4~~	~~3.5~~	~~A~~	~~63/12/25~~	~~92/5/3~~
~~US-MMS~~	~~7.0~~	~~5.2~~	~~I~~	~~69/17/15~~	~~95/4/1~~

~~Site~~	~~H_{can}_default[d] (m)~~	~~H_{can}_site[b] (m)~~	~~S~~	~~I~~	~~PCT_PFT_site[b]~~
~~IT-Cpz~~	~~35~~	~~14.3~~	~~A~~	~~W~~	~~EBT_Tr/DBS_Te/C4 : 50/25/25~~
~~BE-Vie~~	~~17~~	~~33.7~~	~~E~~	~~S~~	~~EBT_Te/C3 : 20/80~~
~~AU-Lit~~	~~35~~	~~20.0~~	~~S~~	~~S~~	~~EBT_Tr/C3/C4 : 10/27/63~~
~~DE-Hai~~	~~20~~	~~33.9~~	~~U~~	~~W~~	~~DBS_Te/C3/C4 : 35/43/22~~
~~IT-Ren~~	~~17~~	~~29.0~~	~~U~~	~~W~~	~~EBT_Te/C3 : 40/60~~
~~DE-Tha~~	~~17~~	~~28.4~~	~~U~~	~~O~~	~~Bare/DBS_Te/C3 : 39/51/10~~
~~IT-Lav~~	~~17~~	~~28.0~~			
~~US-Ton~~	~~20~~	~~9.9~~			
~~RU-Fyo~~	~~17~~	~~26.3~~			
~~CH-Dav~~	~~17~~	~~25~~			

[a] The maximum LAI at the pixel containing the site provided by Reprocessed MODIS version 6.1 LAI. [b] Site-observed data collected in this study. [c] Specific year of maximum LAI. [d] The top layer soil texture (sand/silt/clay) at the site location extracted from the GSDE dataset. ~~[c] Soil texture (sand/silt/clay) at the site location extracted from the GSDE dataset.~~ [~~e~~d] Canopy height of the dominant vegetation type at the site from the CoLM lookup table. ~~[e] Specific year of maximum LAI.~~

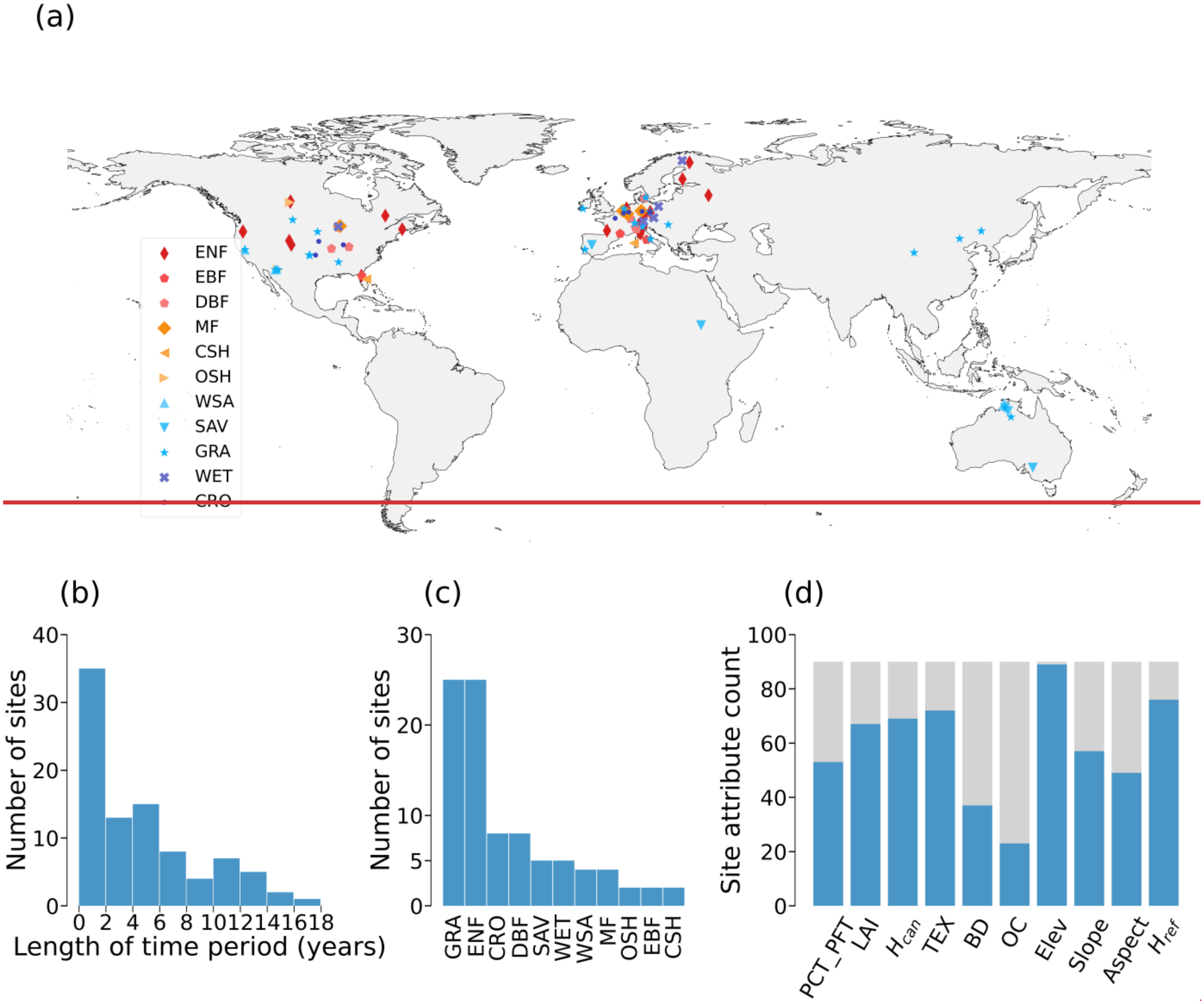
(a)
ENF
EBF
DBF
MF
CSH
OSH
WSA
SAV
GRA
WET
CRO
(b)
Number of sites
Length of time period (years)
(c)
Number of sites
GRA
ENF
CRO
DBF
SAV
WET
WSA
MF
OSH
EBF
CSH
(d)
Site attribute count
PCT_PFT
LAI
H_{can}
TEX
BD
OC
Elev
Slope
Aspect
H_{ref}

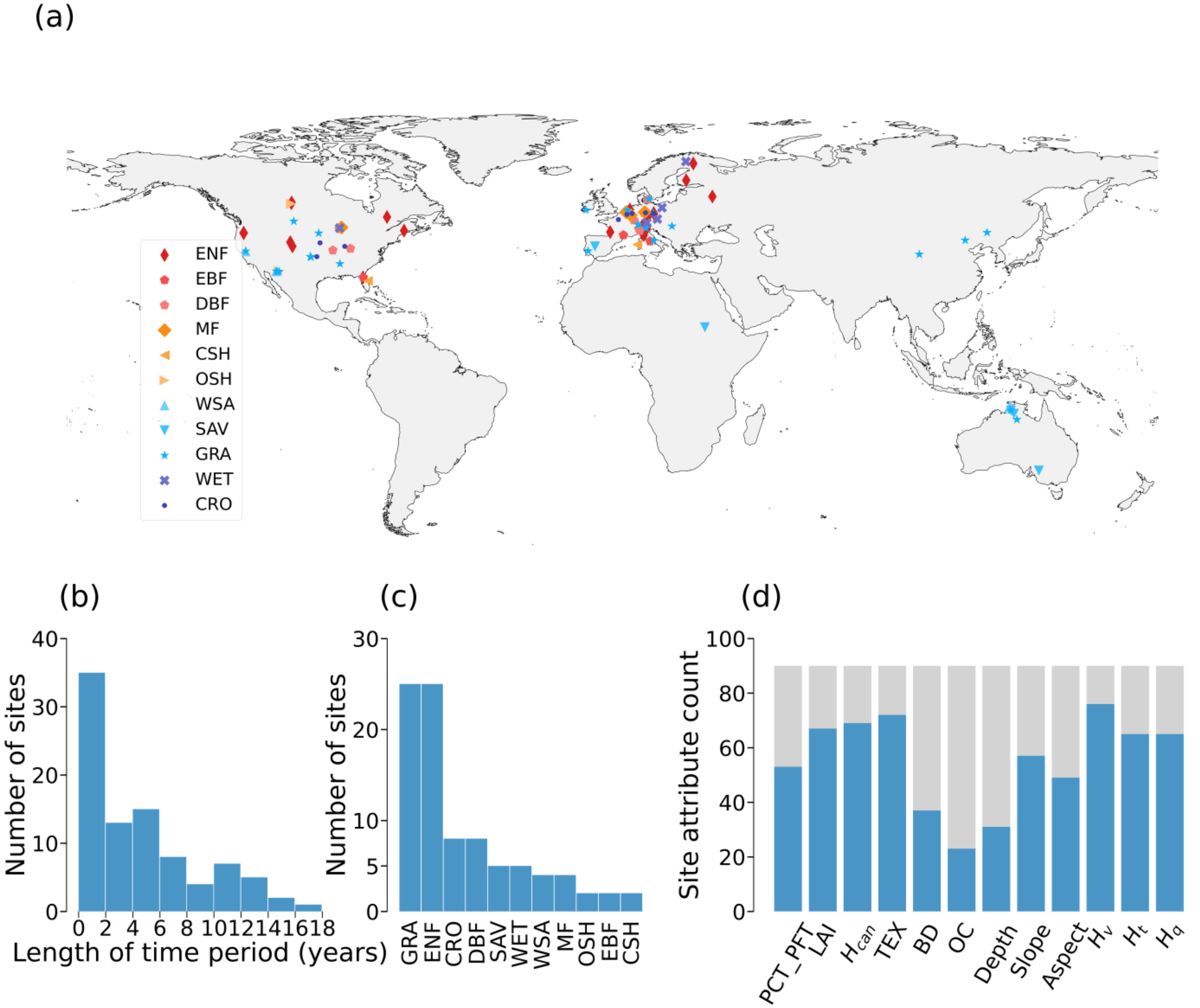

Figure 2. Summary of selected sites and collected site-observed attributes~~ data~~. (a) Geographical distribution~~A map~~ of selected sites and their IGBP types. (b) A histogram showing the number of sites based on the number of years of selected sites data~~numbers for selected sites~~. (c) Number of selected sites per IGBP vegetation class. (d) Number of collected site-observed attributes for percent cover of PFTs (PCT_PFT), maximum LAI (LAI), mean canopy height (H_{can}), soil texture (TEX), bulk density (BD), organic carbon concentration (OC), and soil depth (Depth), slope, aspect, and reference measurement heights (Wind speed: H_v; Air temperature: H_t; Humidity: H_q).~~(d) Number of collected site-observed attribute data for PCT_PFT, maximum LAI (LAI), mean canopy height (H_{can}), soil texture (TEX), bulk density (BD) and organic carbon concentration (OC), elevation (Elev), slope, aspect, and wind reference measurement height (H_{ref}).~~

3 Results

3.1 Global distribution and attribute information of selected sites

The final dataset contains 90 globally distributed sites (Fig. 2a). The majority are in North America and Europe, followed by Australia, with smaller representations in Asia (3 sites) and Africa (1 site). Temporal coverage spans from 1997 to 2017, totaling 475 site years. Individual site observations range from 1 to 17 years, with a median of 4 years (Fig. 2b). Despite a reduction in available sites and years due to rigorous ~~thorough~~ quality control, the dataset does offer reliable meteorological forcing and flux assessment data for LSMs. Furthermore, the 90 sites encompass the full range of IGBP classifications originally presented, covering a wide spread of biomes, from grasslands and savannas to forest ecosystems (Fig. 2c). This enables users to evaluate models across diverse ~~various~~ biomes using quality-benchmarked flux tower observations.

Out of the 90 sites, data were collected on ~~the~~ PCT_PFT for 53 sites, maximum LAI for 67 sites, average canopy height for 69 sites, soil texture for 72 sites, soil bulk density for 37 sites, soil organic carbon concentration~~concentration of soil organic carbon~~ for 23 sites, and soil depth for 31 sites. Data on slope were collected for 57 sites, aspect for 49 sites, wind observation height for 76 sites, and air temperature and humidity observation heights for 65 sites (Fig. 2d). ~~elevation for 89 sites, slope for 57 sites, aspect for 49 sites, as well as wind observation height at 76 sites (Fig. 2d).~~ In the absence of site-observed PCT_PFT, soil texture~~TEX~~, and LAI, we opted for appropriate global data to ~~complement~~ fill in these missing ~~them~~ for data completeness. To improve data utilization, we provide ~~offer~~ the observation year of maximum LAI and the depth of soil texture, which are available~~were availed~~ at 33 and 34 sites, respectively.

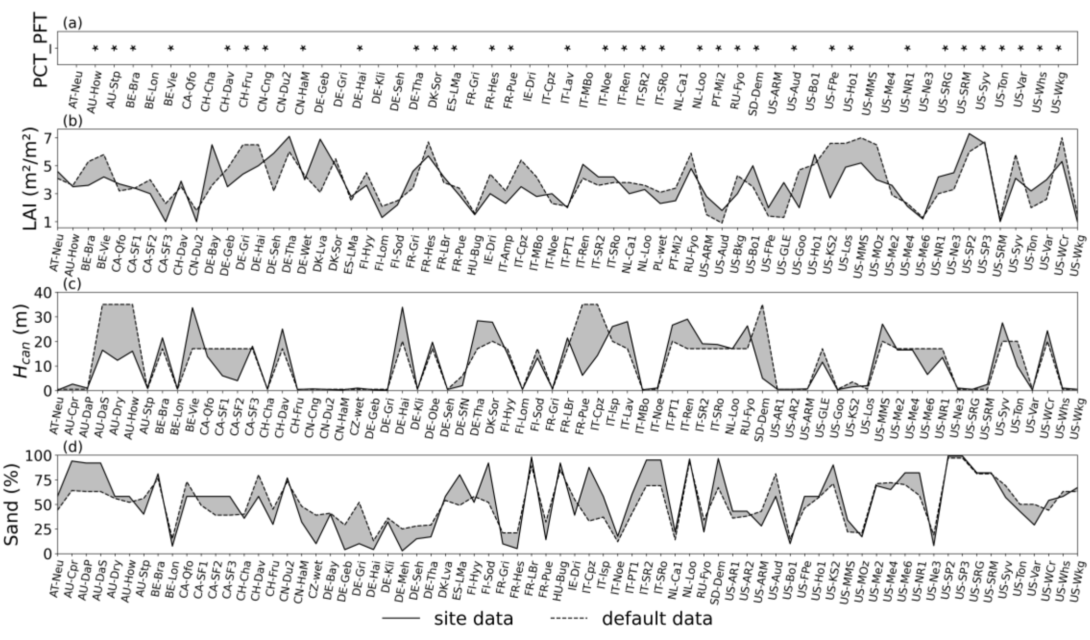

Figure 3. The discrepancies between site data and default data of (a) percent cover of PFTs (PCT_PFT), ~~(~~the asterisk indicates non-single PFTs~~)~~, (b) maximum LAI, (c) canopy height (H_{can}), and (d) the percentage of sand.

Figure 3 depicts the discrepancies between site data and default data for PCT_PFT, maximum LAI, canopy height, and soil texture. The PCT_PFT shows multiple~~has non-single~~ PFTs at 34 sites, offering a more accurate representation of ~~the~~ vegetation conditions compared to IGBP classifications. ~~As f~~For LAI, canopy height, and soil texture, variations between site data and default data are substantial ~~in~~ at certain sites. Specifically, at 31 sites, discrepancies in LAI values exceed 1 m^2/m^2; canopy height differs by over 10 meters at 15 sites, and sand percentage varies by more than 20% at 18 sites.~~Specifically, at 31 sites, there is a discrepancy in LAI values exceeding 1 m^2/m^2, and canopy height differing by over 10 meters at 15 sites, with the disparity in sand % exceeding 20 % at 18 sites.~~

3.2 The flux tower site attribute dataset

The final dataset is formatted in NetCDF (Network Common Data Form). Table 3 outlines the attribute variables and corresponding ~~supporting~~ descriptions for each site in the file. These attributes can be categorized into vegetation, soil, and topography attributes, as well as reference heights~~,~~ and filtered high-quality years.

For ~~the~~ maximum LAI, the file provides both the year range covered by~~furnishes the range of years for~~ maximum LAI~~,~~ and the maximum value for a specific year. Regarding the three soil attributes, soil texture, bulk density, and organic carbon concentration, the file provides ~~attribute~~ values for multiple soil layers, along with the specific depth of each layer.~~and gives the specific depth of their corresponding soil layer.~~ Concerning reference height, we give its corresponding observed variable, i.e., wind speed or fluxes (latent and sensible heat). Additionally, the NetCDF file incorporates reference sources for each attribute. These sources are included to facilitate access to the original data and enhance flexibility in application. A ~~comprehensive~~ summary of these reference sources is presented ~~provided~~ in Table S1.

Table 3. Attribute variables and their ~~auxiliary~~ descriptions included ~~provided~~ in the final dataset (note that not all sites provide ‘Soil_BD’, ‘Soil_OC’, ‘Soil_depth’, ‘Slope’, and ‘Aspect’).

Variable (Dimension)	Long name	Unit	Description
PCT_PFT (pft=16)	Percent plant functional types cover	%	Source[a];
LAI_Max	Maximum leaf area index	m^2/m^2	Source; year_range[b]; LAI_Max_year[c]
Canopy_height	Canopy height	m	Source;
Soil_TEX (particle_size=3, soil_layer=4)	Soil texture(sand/silt/clay)	%	Source; layer_n_depth[d]
Soil_BD (soil_layer=4)	Soil bulk density	$g\ cm^{-3}$	Source; layer_n_depth[d]
Soil_OC (soil_layer=4)	Soil organic carbon concentration	%	Source; layer_n_depth[d]
Soil_depth	Soil depth	cm	Source
~~Elevation~~	~~Site elevation~~	~~m~~	~~Source;~~
Slope	Site slope	-	Source;
Aspect	Site aspect	-	Source;
Reference_height_v	Measurement height of wind speed or flux	m	Source; Measurement variable (Wind or Flux)
Reference_height_t	Measurement height of air temperature or flux	m	Source; Measurement variable (Temperature or Flux)

Reference_height_q	Measurement height of air humidity or flux	m	Source; Measurement variable (Humidity or Flux)
year_qc (year=21)	Selected year of high-quality data	-	-

[a] The sources of collected attribute data. [b] The year range covered by~~Range of years with~~ maximum LAI. [c] Maximum LAI for specific year. [d] The "n" ranges from 1 to 4, denoting the four soil layers in ascending order of depth. The parameter "layer_n_depth" indicates the depth of respective "soil layer", corresponding to the depth at which soil data is observed.

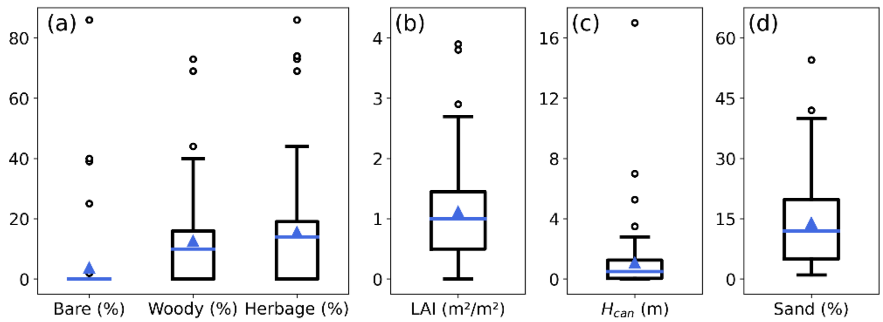

Figure 4. Quantification of discrepancies between site data and filled data for (a) PCT_PFT, (b) maximum LAI, (c) canopy height, and (d) percentage of sand (at all sites for which both types of data are available). The 16 PFTs were divided into three main categories (bare soil, woody, and herbaceous vegetation) for separate quantification.

Figure 4 quantifies the differences between site data and filled data for sites where both data sources are available, illustrating the inhomogeneities in the final dataset resulting from data filling. Differences in vegetation cover (including bare soil, woody, and herbaceous vegetation) generally fall within 20 %, with a minority of sites exceeding 40 %. The mean and median LAI differences are approximately 1 m2/m2. Canopy height deviations are primarily within 2 m, although a few sites exceed 4 m. Differences in sand content typically remain within 30%, with both mean and median differences below 15 %. This quantification suggests that the filled data are generally reliable across most sites.

3.3 Impact of site attributes on modeling

The impacts of altering land surface representation from default data to site data, quantified by MD %, on ~~LE~~Qle, Qh~~H~~, Rn, SWup, GPP, Ustar, SWC, and TR are shown in Fig. 5~~4~~. It distinctly demonstrates how vegetation and soil components affect carbon, water, and energy fluxes to varying degrees, contingent on the season. The impacts ~~influence~~ of vegetation cover, soil texture, and LAI on Qle~~LE~~ and Qh~~H~~ is primarily observed ~~felt~~ in the spring and summer, while canopy height exerts its most substantial effects in autumn and winter.~~. The opposite was true for canopy height, which produced the most substantial effects in autumn and winter.~~ The impact of vegetation cover on Rn and SWup remains ~~more~~ consistent throughout the year, whereas LAI maintains a more pronounced effect in spring and summer. In terms of GPP, attributes ~~factors~~ play a more significant role during the summertime. ~~But~~ However, the effects of vegetation and soil on attributes Ustar appear to be independent of season. ~~For~~ SWC and TR are~~,~~ both ~~are~~ predominantly influenced by soil texture. The difference is that soil texture significantly affects SWC across all seasons, whereas its impact on TR occurs primarily during the summer and fall. Additionally, ~~it was noted that~~ vegetation cover was observed to ~~could~~ have a significant effect ~~change~~ on TR at the SD-Dem site. This is due to the salient impact at the SD-Dem site, situated within the African savannah with an average annual precipitation of 320 mm (Ardö et al., 2008).

To elucidate the magnitude of each attribute's impact on different variables, figure 6~~5~~ further displays the monthly average maximum MD %. On average, changes in latent and sensible heat are not dominated by any single attribute. All four attributes —PCT_PFT, LAI, canopy height, and soil texture—have a relatively strong impact on both.~~the impacts of four attributes—PCT_PFT, LAI, canopy height, and soil texture—on LE and H were comparatively equilibrated.~~ Their monthly average maximum MD % on Qh~~H~~ ~~are~~ is all in the range of 14-36~~15-30~~ %. And the effect of soil texture on Qle~~LE~~ is comparatively ~~relatively significant~~greater, at 18.3 %~~17.5 %~~. ~~Moving on to~~Regarding Rn, vegetation cover emerges as the chief influencer with a monthly average maximum MD % of ~~8.5~~8.8 %. In contrast, SWup is heavily dictated by LAI, at 56.7~~52.8~~ %, due to~~because of~~ the exceptionally high value at the US-GLE site. ~~The v~~Vegetation cover and LAI, both with a monthly average maximum MD % of more than 50 %, dominate the changes in ~~of~~ GPP. Soil texture also has a visible impact on GPP, due to its influence on soil~~Since soil texture affects~~ permeability, aeration, and the the capacity to retain~~ability of the soil to hold~~ water and nutrients~~, it also has a visible impact on GPP~~. On the other hand, Ustar is almost exclusively shaped by vegetation cover and canopy height. This makes sense because the intensity of land-atmosphere exchange in vegetated areas is directly tied to canopy height, and changes in vegetation cover typically correspond to changes in canopy height. Concerning SWC and TR, vegetation cover and soil texture are the two crucial attributes. Soil texture exhibits ~~exhibited~~ monthly average maximum MD % of 46.3~~46.8~~ % for SWC and ~~147.9~~129.8 % for TR ~~each~~, while vegetation cover shows~~ed~~ 22.7~~22.6~~ % and ~~278.8~~293.8 %, respectively.

Figure 7~~6~~ uses ΔRMSE and Δ|Bias| to show the shifts in model performance using site data. The incorporation of site-observed attribute data significantly improves the simulation of Rn, SWup, and Ustar. ~~Specifically~~ Concerning~~with respect to~~ individual attributes, ~~the~~ PCT_PFT proves particularly beneficial~~helpful~~ for modeling both Rn and SWup. Concurrently, the inclusion of site LAI also enhances the simulation~~contributes to the enhancement~~ of SWup. Improvements in~~Enhancements to~~ these fundamental energy terms contribute to more accurate modeling of latent and sensible heat. Furthermore, ~~the use of~~ site LAI and canopy height demonstrates steady improvements on GPP and Ustar, respectively.

In summary, these results underscore the significant impact and importance of incorporating site-observed attribute data in the simulation of carbon, water, and energy fluxes in LSMs.

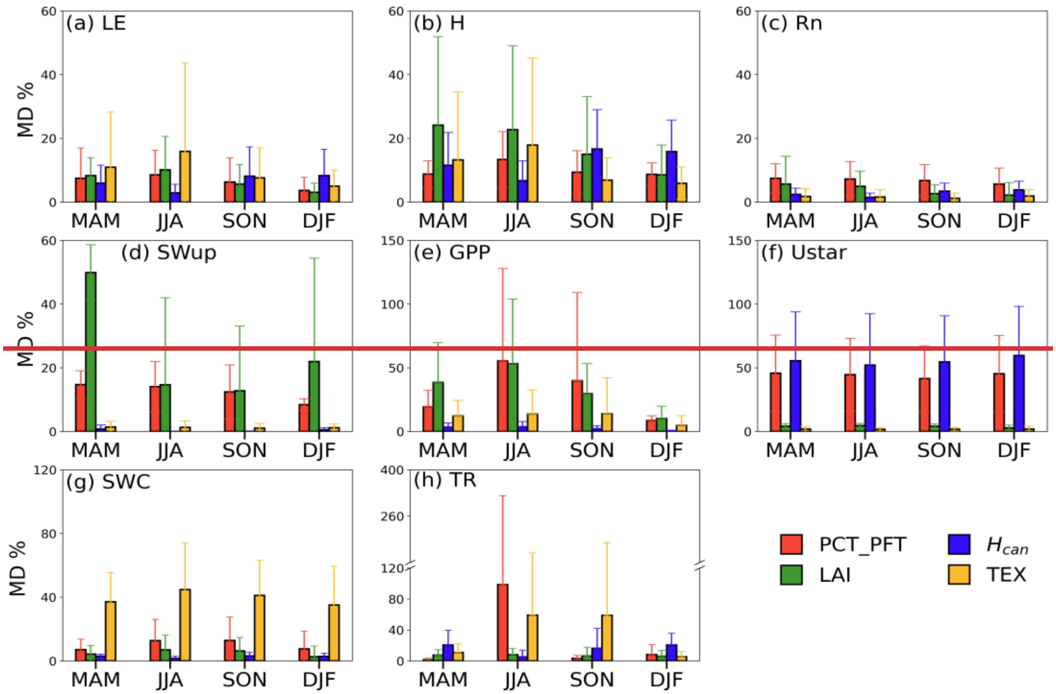

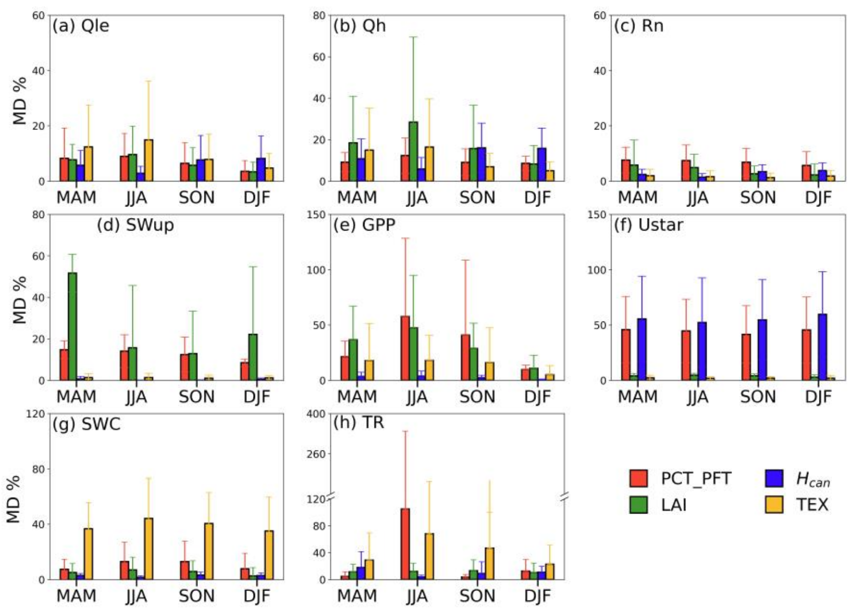

Figure 4. Percentage~~The percentage~~ of mean difference (MD %) of PCT_PFT, LAI, canopy height (H_{can}) and soil texture (TEX) on Qle~~LE~~, Qh~~H~~, Rn, SWup, GPP, Ustar, SWC and TR for each season, respectively. Error~~The error~~ bars indicate one ~~a~~ standard deviation from the multi-site mean. Monthly adjustments were made for S~~s~~outhern H~~h~~emisphere sites~~ in calculations~~, to ensure consistency between seasons and months in multi-site averaging (i.e., DJF ~~are~~ is considered ~~to be~~ JJA, MAM ~~are~~ is considered ~~to be~~ SON, and vice versa~~so on.~~).

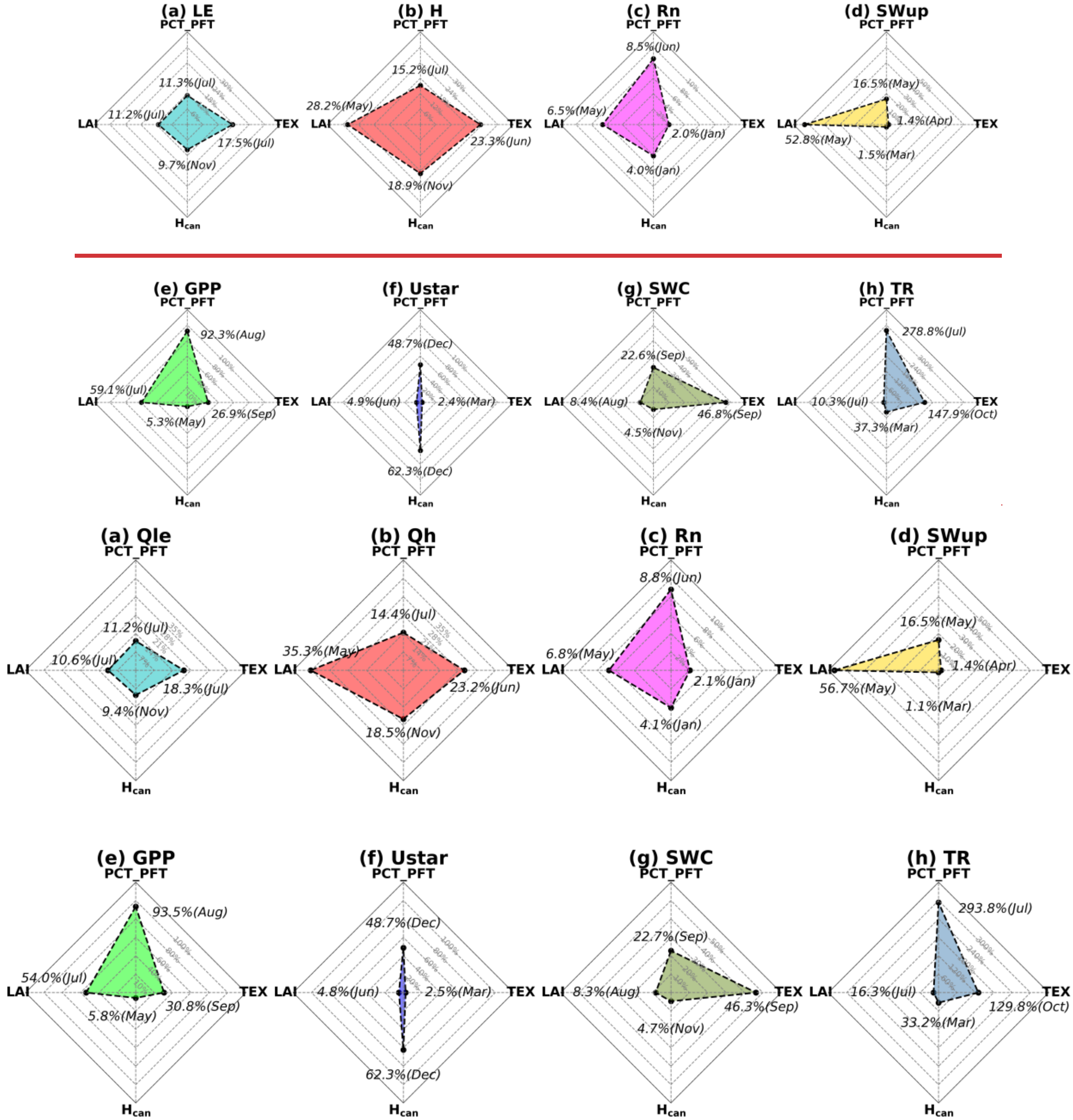

Figure 5. ~~The m~~Monthly average maximum MD % of PCT_PFT, LAI, canopy height (H_{can}) and soil texture (TEX) on Qle~~LE~~, Qh~~H~~, Rn, SWup, GPP, Ustar, SWC and TR, respectively. The month of occurrence for each~~with the~~ maximum value is indicated in parentheses.

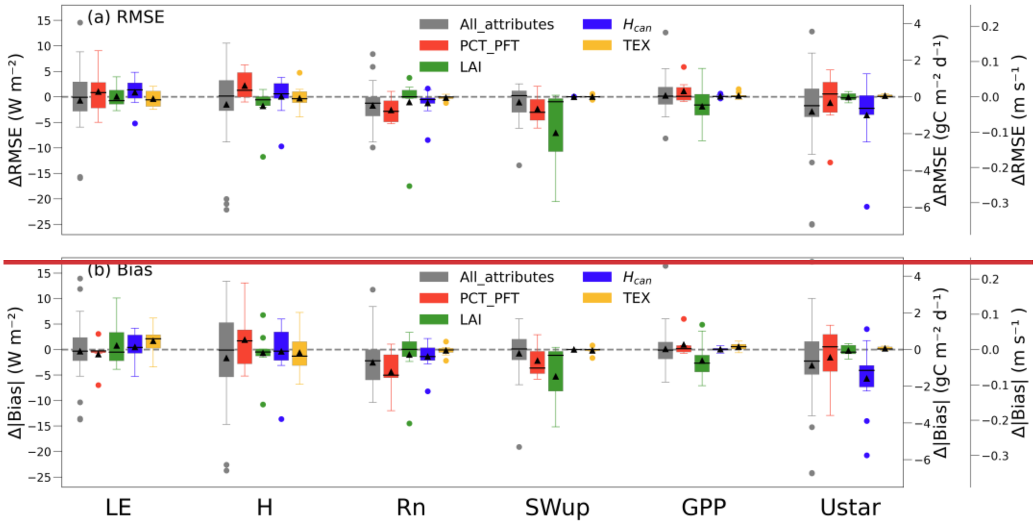

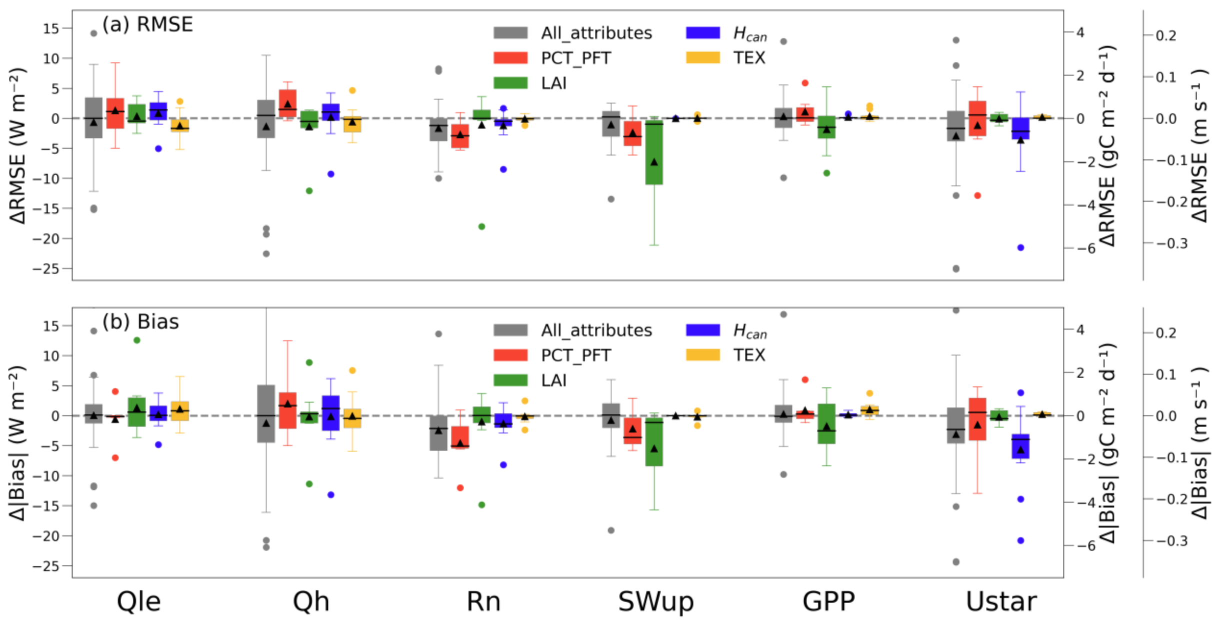

Figure 6. Box plot of changes in RMSE (ΔRMSE) and absolute Bias (Δ|Bias|) when using site data versus default data. PCT_PFT, LAI, H_{can} (~~Canopy~~ canopy height), and TEX (soil texture) denote the individual impacts of the four attributes. All_attributes represents the changes produced by four attributes together across the 36 sites selected. Boxes (25th and 75th percentiles) and whiskers (5th and 95th percentiles), with median (black line) and mean (black triangle). Solid circles denote outliers defined as ~~for~~ values greater than 1.5 times the interquartile range from the nearest 25th or 75th percentile.

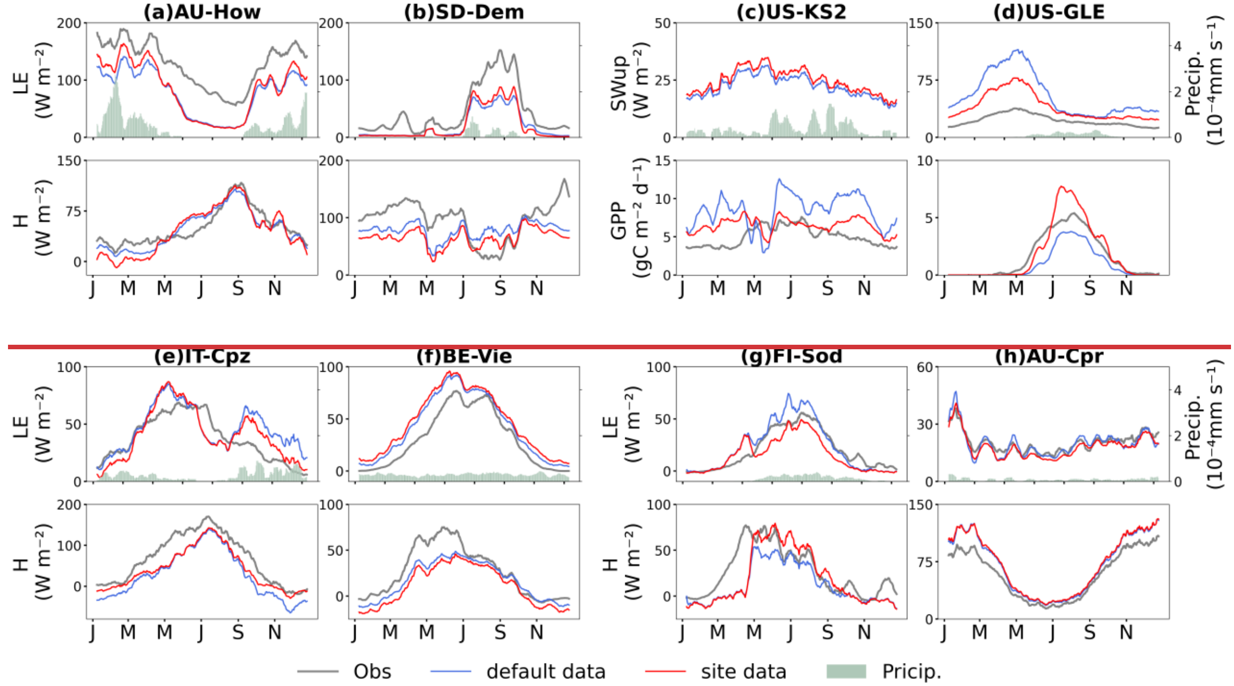

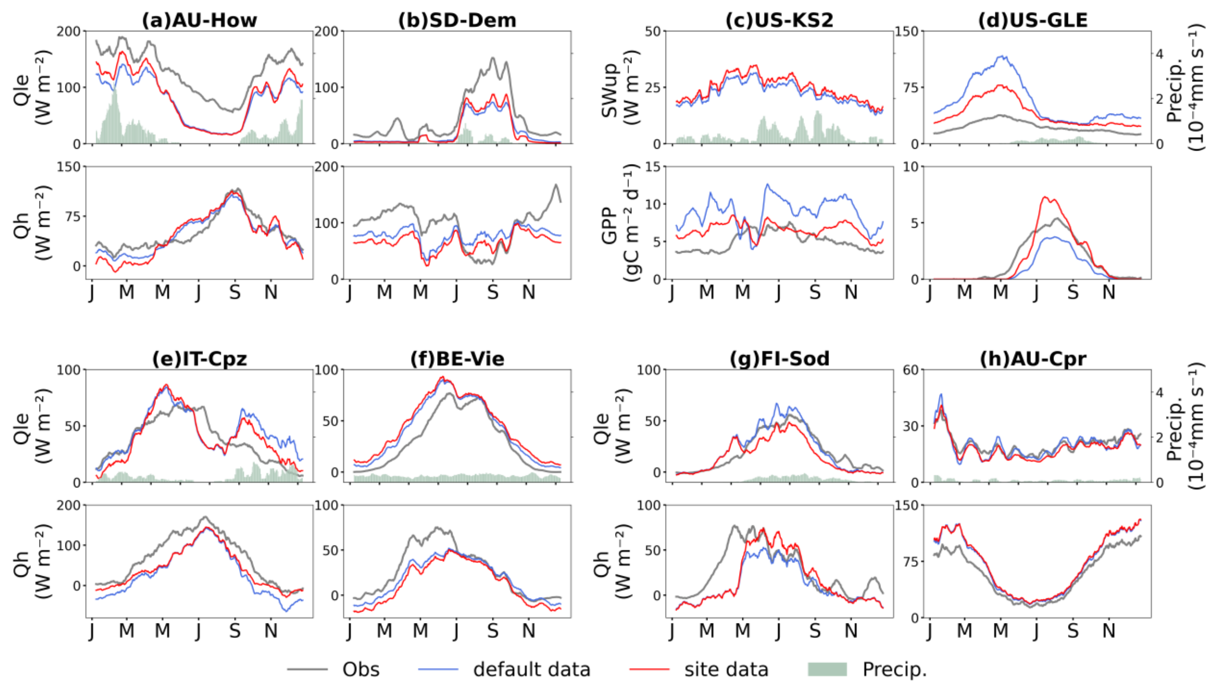

Figure 7. Multi-year daily average of the seasonal cycle of model (default, site) and observed Qle~~LE~~, Qh~~H~~, SWup, and GPP at 8 selected sites, Two sites were chosen for each attribute for comparison: PCT_PFT (AU-How and SD-Dem), LAI (US-

KS2 and US-GLE), H_{can} (IT-Cpz and BE-Vie), Soil texture (FI-Sod and AU-Cpr).~~,~~ Data are smoothed with a 14-day moving average for clarity.

4 Discussion

In land surface community, flux tower attribute data ~~is~~ currently does not receive sufficient~~given enough~~ attention. However, the site attribute data are nearly as critical as the flux tower observations themselves. We hope that future flux tower datasets will provide standardized site attributes. In this study, we have acquired 90 sites with high quality by a comprehensive selection process, and providing extensive site-observed data on vegetation, soil, and topography attributes.~~Here, we have acquired 90 sites with dependable quality by comprehensive selection, and provided data on vegetation, soil, and topography attributes observed at the site.~~ Through single-point simulations, we demonstrated ~~illustrated~~ their indispensable role in LSM development. Accurate attribute data will provide multiple benefits by lowering uncertainty in model ~~single-point~~ calibration and evaluation.

After selection, fewer sites and years are available. However, the retained data offers trustworthy observations that can be directly applied. Data quality is generally the focus of model calibration and evaluation, and developing LSMs can benefit immensely from using~~the usage of~~ a modest number of sites (Brooke et al., 2019; Harper et al., 2021; Swenson et al., 2019). Therefore, these updates will help the model's developments.~~These updates will therefore help the model's evolution.~~ To collect more site-observed attribute data, while considering~~taking into account~~ the diversity described within the same attribute data, particularly the percentage of vegetation cover,~~. W~~we made a few approximations and assumptions during~~in the~~ data collection procedure, such as using approximation substitution and site photographs to assist in judgment.~~.~~ Although these methods may introduce slight deviations~~ from the genuine values~~, they do a good job of reproducing the surface conditions of these sites. Furthermore, we provide descriptions of the attribute data as detailed as possible. For instance, the year and depth of observation are given along with the maximum LAI and soil texture whenever feasible, respectively. They are valuable references for data applications. One might argue that the auxiliary descriptions are just as important as the attribute data itself.

Using CoLM at 36 sites, we evaluated the impacts of PCT_PFT, LAI, canopy height, and soil texture on model results. What is conducted here is not an ideal experiment, but rather an actual demonstration of the discrepancies in model results between site data and default data. The results are in line with previous research (Dai et al., 2019a), showing that vegetation cover appreciably affects each of the eight variables examined, often being the dominant attribute (Fig. 6). This is due to plant cover being the most prominent surface feature, directly altering surface energy absorption. The net radiation simulation was improved using the site PCT_PFT, but the performance of latent and sensible heat was not as good. This may be related to uncertainties in the model itself as well as other input data. Such as vegetation biophysical parameters, soil thermal and hydraulic conductivities, etc.~~According to the results, which are in line with earlier research (Dai et al., 2019b), vegetation cover appreciably affects each of the eight variables examined. And among the four attributes, net radiation was~~

~~the most affected by vegetation cover (Fig. 5). This is due to the cover of plants being the most noticeable surface feature, directly changing surface energy absorption. The net radiation simulation was enhanced using the site PCT_PFT, but the latent and sensible heat did not perform as well. This may be related to the model's previous development and evaluation, which was mostly centered on the IGBP classifications (Dai et al., 2019c; Zhang et al., 2017; Zhu et al., 2017). Notably, unit LAI variations elicit more substantial fluctuations in fluxes at lower LAI values (usually less than 2 m^2/m^2), according to Launiainen et al. (2016). In light of that, all of the sites we chose have LAI values greater than 2 m^2/m^2, except US-GLE, the impact of LAI obtained here are relatively minor.~~

Additionally, we find that the impact of attributes is substantially associated with precipitation. As illustrated in the average seasonal cycle shown in Fig. 8~~7~~.~~,~~ At the AU-How site in Australia~~ along with~~, ample rainfall during the wet season, ~~and~~ combined with the increase in surface available energy due to vegetation cover, brings about a significant increase in Qle~~LE~~. In contrast, since limited water is available for evapotranspiration at the SD-Dem site, ~~H~~ Qh is the primary feedback from changes in surface energy. The results from the US-KS2 and US-GLE sites indicate that the growing season, synchronized with water availability, is when LAI exerts a major influence on GPP. Furthermore, ~~And~~ a notable variation in SWup was seen at the US-GLE site, attributed to the presence of snow cover (Berryman et al., 2018). Corrections to LAI can improve the simulation by reducing albedo inaccuracies. This corroborates ~~the~~ Essery (2013) point that inadequate land-cover data ~~was~~ is largely to blame for the uncertainty in the climate–snow albedo feedback in LSMs. Results from the IT-Cpz and BE-Vie sites suggest that differences in the intensity of land-air exchange, caused by variations in canopy height, are clearly ~~truly~~ reflected in Qle~~LE~~ during the rainy season. Regarding soil texture, a comparison~~ of results~~ between FI-Sod and AU-Cpr sites revealed stronger control of Qle~~LE~~ by soil texture during the period of high precipitation intensity. This is partly attributed to increased water availability and largely to the pronounced differences in soil infiltration capacity under high-intensity precipitation events.~~the full realization of differences in soil infiltration capacity under high-intensity precipitation.~~

A previous study by Ménard et al. (2015)~~viewed~~ stated that attribute data have little effect on modeling results~~ (Ménard et al., 2015)~~. ~~Its~~ This study, however, may lack representativeness since it was limited to one site. Furthermore, it averaged differences resulting from attribute data across the whole time series, by using the raw RMSE and correlation coefficient statisticals~~s~~ metrics. This approach ~~does~~ makes it difficult to detect the crucial role of attribute data. As described in Sect. 3.3, the impacts of attribute data on climate-related variables generally occur over specific periods (mostly during the growing season) rather than throughout the year~~occur mostly during the growing season~~.

By combining multiple data sources, we were able to maximize the available site-observed attribute data. Nevertheless, the data sources were primarily from published works, which led to some missing data at certain sites. The attribute data focused only on soil and vegetation information.~~Nevertheless, the data sources were published works, leading to deficiencies for certain sites. And the attribute data we collected focused on fundamental soil and vegetation information.~~ Future endeavors should incorporate~~will call for the incorporation of~~ additional surface parameters, such as irrigation, wildfire, and the depth of soil moisture and vegetation roots, which are required ~~demanded~~ for LSMs. Such observations and collections of site time-invariant attributes are generally low-cost but would strongly benefit model enhancement.~~These collections of site attributes are low-cost but would strongly benefit model enhancement.~~ In addition, the impact of attribute data on model results was assessed ~~simulated~~ using one model, potentially limiting the representativeness of our findings.

As LSMs continually advance~~s its~~ their schemes and processes, an increasing array of surface parameters will be incorporated, elevating the models to a heightened level of ~~sophistication~~complexity. It is imperative that these parameters be clearly defined and prescribed~~clarified~~. Working with site-observed attribute data enabled us to narrow down reasons for model biases, thereby enhancing our understanding of the true effects of diverse schemes and processes.~~facilitating perception of the authentic feedback with diverse schemes and processes.~~

5 Data availability

The flux tower site attribute dataset provides comprehensive filtered high-quality years, site-observed vegetation, soil, topography attributes, and reference measurement height. Each site's data is formatted within a NetCDF file named according to the site name, database, and attributes (vegetation, soil, topography, and reference height), such as 'AT-Neu_FLUXNET2015_Veg_Soil_ Topography_ReferenceHeight.nc'. The dataset comprises a total of 90 NetCDF files and can be accessed at Zenodo under https://doi.org/10.5281/zenodo.12596218~~https://doi.org/10.5281/zenodo.10939725~~ (Shi et. al., 2024).

6 Code availability

The processing codes are available at https://github.com/Mbnl1197/Flux-tower-attribute-for-LSM (last access: 2 March 2024) (DOI: https://doi.org/10.5281/zenodo.10939950; Shi et. al., 2024)

7 Conclusions

This study is centered on two issues with utilizing flux tower data in LSMs~~, including~~: inadequate data quality ~~of data~~ and insufficient site attributes~~ data~~. We performed a comprehensive quality control on flux tower data. By examining~~Through the examination of~~ observation percentage, energy balance closure, and external disturbances, 90 high-quality flux tower sites with 475 site years were produced. By ~~C~~combining various data sources, we created a flux tower attribute dataset through data collection, processing, and ~~complementarity~~filling procedures. This dataset includes ~~. T~~the site-observed PCT_PFT, maximum LAI, mean canopy height, soil properties (texture, bulk density, organic carbon concentrations, and depth), site topography (slope and aspect), as well as the reference measurement heights. ~~soil texture, bulk density and organic carbon concentrations, site elevation, slope and aspect were collected, and wind speed measurement height~~ was acquired.

Furthermore, the attribute data collected in this study and frequently used by LSMs are incorporated in single-point modeling respectively, aimed at quantifying the differences in model output. Our results demonstrate the significance of certain attributes in the variation of specific variables. All four attributes significantly influence both latent and sensible heat. Their monthly average maximum MD % typically ranges from 10 % to 30 %. Vegetation cover and LAI serve as the primary controls for net radiation and upward shortwave radiation, respectively, with monthly average maximum MD % of 8.8~~8.5~~ % and 56.7~~52.8~~ %. Both GPP and Ustar were strongly influenced by vegetation cover, with LAI and canopy ~~tree~~ height also exerting significant effects on GPP and Ustar, respectively. The monthly average maximum MD % for each of these impacts exceeds 50 %. For hydrologic variables, i.e., SWC and TR, soil texture typically holds greater significance, followed by vegetation cover. We reveal that the magnitude of these differences is usually accompanied by seasonal fluctuations. Particularly regarding fluxes and GPP, greater discrepancies are generally observed ~~discerned~~ during spring and summer. These results stress the necessity of site-observed attribute data in the development of LSMs.

Our endeavors mitigate the inadequacies of flux tower attribute data, enhancing ~~elevating~~ the ability of flux tower data to serve as benchmarking data for LSMs. The dataset provides relatively complete site attribute data and high-quality flux validation data, making it suitable for direct use as inputs and for simulation validation in LSMs~~which can be directly used as inputs and simulation validation for LSMs~~. This facilitates the comparison of LSM simulations under the same standard framework, promoting their development. Moreover, this effort will draw more attention to flux tower attribute data from the land surface modeling ~~community~~ group and foster communication between ecology and modeling communities. We strongly advocate for the routine release of attribute data as part of flux tower data. Making such ancillary data more easily and routinely accessible would greatly increase the value and usability of the data.

Author contributions

Conceptualization: H.Y.; Data curation: H.Y. and J.S.; Formal analysis: J.S., H.Y., W.D. and W.L.; Funding acquisition: H.Y. and Y.D.; Investigation: H.Y. and J.S.; Methodology: H.Y., J.S., N.W., Z.W. and S.L.; Resources: Y.D. and H.Y.; Software: J.S., H.Y., H.L., W.L., N.W., J.Z. and H.Z.; Validation: H.Y., Z.L., W.D., W.L., S.Z. and X.L.; Visualization: J.S.; Writing – original draft preparation: J.S.; Writing – review & editing: J.S., H.Y., Z.W., W.L., W.D., Z.L. and Y.D. All authors have read and agreed to the published version of the manuscript.

Competing interests

The authors declare that they have no conflict of interest.

Acknowledgements

We thank Anna M. Ukkola for her solid work in flux tower data processing, which provided a robust foundation for our research. We are also grateful for her responsiveness to our questions in using PLUMBER2. We extend our thanks to

Danielle Svehla Christianson of Integrated Data Systems, Scientific Data Division, and Lawrence Berkeley National Laboratory for her prompt assistance in utilizing AmeriFlux BADM data. This work accessed several flux tower networks in the FLUXNET community, including AmeriFlux, ChinaFlux, European Fluxes, OzFlux, and Swiss Fluxnet. Special thanks to FLUXNET and AmeriFlux for providing the BADM data. We also accessed data from ESRL's Global Monitoring Laboratory (GML) of the National Oceanic and Atmospheric Administration (NOAA) and the AT-Neu site research group. This work is based on numerous publications, we thank these scientists for sharing their data. The PFT_{local} maps were supported and provided by the ESA CCI Land Cover project. The Köppen-Geiger climate classification maps are hosted by GloH2O.

Financial support

This work was supported by the Natural Science Foundation of China (under Grants 42075160 and 42088101), Guangdong Major Project of Basic and Applied Basic Research (2021B0301030007), the Southern Marine Science and Engineering Guangdong Laboratory (Zhuhai) (No. SML2023SP216) and the specific research fund of The Innovation Platform for Academicians of Hainan Province (YSPTZX202143).

References

Anderson, R. G., Canadell, J. G., Randerson, J. T., Jackson, R. B., Hungate, B. A., Baldocchi, D. D., Ban-Weiss, G. A., Bonan, G. B., Caldeira, K., Cao, L., Diffenbaugh, N. S., Gurney, K. R., Kueppers, L. M., Law, B. E., Luyssaert, S., and O'Halloran, T. L.: Biophysical considerations in forestry for climate protection, Frontiers in Ecol & Environ, 9, 174–182, https://doi.org/10.1890/090179, 2011.

Ardö, J., Mölder, M., El-Tahir, B. A., and Elkhidir, H. A. M.: Seasonal variation of carbon fluxes in a sparse savanna in semi arid Sudan, Carbon Balance Manage, 3, 7, https://doi.org/10.1186/1750-0680-3-7, 2008.

Arya, L. M. and Paris, J. F.: A physicoempirical model to predict the soil moisture characteristic from particle-size distribution and bulk density data, Soil Science Society of America Journal, 45, 1023–1030, https://doi.org/10.2136/sssaj1981.03615995004500060004x, 1981.

Bagley, J. E., Kueppers, L. M., Billesbach, D. P., Williams, I. N., Biraud, S. C., and Torn, M. S.: The influence of land cover on surface energy partitioning and evaporative fraction regimes in the U.S. Southern Great Plains, JGR Atmospheres, 122, 5793–5807, https://doi.org/10.1002/2017JD026740, 2017.

Beck, H. E., Zimmermann, N. E., McVicar, T. R., Vergopolan, N., Berg, A., and Wood, E. F.: Present and future Köppen-Geiger climate classification maps at 1-km resolution, Sci Data, 5, 180214, https://doi.org/10.1038/sdata.2018.214, 2018.

Berryman, E. M., Vanderhoof, M. K., Bradford, J. B., Hawbaker, T. J., Henne, P. D., Burns, S. P., Frank, J. M., Birdsey, R. A., and Ryan, M. G.: Estimating soil respiration in a subalpine landscape using point, terrain, climate, and greenness data, JGR Biogeosciences, 123, 3231–3249, https://doi.org/10.1029/2018JG004613, 2018.

Best, M. J., Abramowitz, G., Johnson, H. R., Pitman, A. J., Balsamo, G., Boone, A., Cuntz, M., Decharme, B., Dirmeyer, P. A., Dong, J., Ek, M., Guo, Z., Haverd, V., van den Hurk, B. J. J., Nearing, G. S., Pak, B., Peters-Lidard, C., Santanello, J. A., Stevens, L., and Vuichard, N.: The Plumbing of Land Surface Models: Benchmarking Model Performance, Journal of Hydrometeorology, 16, 1425–1442, https://doi.org/10.1175/JHM-D-14-0158.1, 2015.

Blyth, E., Gash, J., Lloyd, A., Pryor, M., Weedon, G. P., and Shuttleworth, J.: Evaluating the JULES Land Surface Model Energy Fluxes Using FLUXNET Data, Journal of Hydrometeorology, 11, 509–519, https://doi.org/10.1175/2009JHM1183.1, 2010.

Bonan, G. B.: Forests and Climate Change: Forcings, Feedbacks, and the Climate Benefits of Forests, Science, 320, 1444–1449, https://doi.org/10.1126/science.1155121, 2008.

Bonan, G. B., Levis, S., Kergoat, L., and Oleson, K. W.: Landscapes as patches of plant functional types: An integrating concept for climate and ecosystem models, Global Biogeochem. Cycles, 16, 5-1-5–23, https://doi.org/10.1029/2000GB001360, 2002.

Brooke, J. K., Harlow, R. C., Scott, R. L., Best, M. J., Edwards, J. M., Thelen, J.-C., and Weeks, M.: Evaluating the Met Office Unified Model land surface temperature in Global Atmosphere/Land 3.1 (GA/L3.1), Global Atmosphere/Land 6.1 (GA/L6.1) and limited area 2.2 km configurations, Geosci. Model Dev., 12, 1703–1724, https://doi.org/10.5194/gmd-12-1703-2019, 2019.

Chu, H., Luo, X., Ouyang, Z., Chan, W. S., Dengel, S., Biraud, S. C., Torn, M. S., Metzger, S., Kumar, J., Arain, M. A., Arkebauer, T. J., Baldocchi, D., Bernacchi, C., Billesbach, D., Black, T. A., Blanken, P. D., Bohrer, G., Bracho, R., Brown, S., Brunsell, N. A., Chen, J., Chen, X., Clark, K., Desai, A. R., Duman, T., Durden, D., Fares, S., Forbrich, I., Gamon, J. A., Gough, C. M., Griffis, T., Helbig, M., Hollinger, D., Humphreys, E., Ikawa, H., Iwata, H., Ju, Y., Knowles, J. F., Knox, S. H., Kobayashi, H., Kolb, T., Law, B., Lee, X., Litvak, M., Liu, H., Munger, J. W., Noormets, A., Novick, K., Oberbauer, S. F., Oechel, W., Oikawa, P., Papuga, S. A., Pendall, E., Prajapati, P., Prueger, J., Quinton, W. L., Richardson, A. D., Russell, E. S., Scott, R. L., Starr, G., Staebler, R., Stoy, P. C., Stuart-Haëntjens, E., Sonnentag, O., Sullivan, R. C., Suyker, A., Ueyama, M., Vargas, R., Wood, J. D., and Zona, D.: Representativeness of Eddy-Covariance flux footprints for areas surrounding AmeriFlux sites, Agricultural and Forest Meteorology, 301–302, 108350, https://doi.org/10.1016/j.agrformet.2021.108350, 2021.

Crow, W. T., Kumar, S. V., and Bolten, J. D.: On the utility of land surface models for agricultural drought monitoring, Hydrol. Earth Syst. Sci., 16, 3451–3460, https://doi.org/10.5194/hess-16-3451-2012, 2012.

Dai, Y., Zeng, X., Dickinson, R. E., Baker, I., Bonan, G. B., Bosilovich, M. G., Denning, A. S., Dirmeyer, P. A., Houser, P. R., Niu, G., Oleson, K. W., Schlosser, C. A., and Yang, Z.-L.: The Common Land Model, Bulletin of the American Meteorological Society, 84, 1013–1024, https://doi.org/10.1175/BAMS-84-8-1013, 2003.

Dai, Y., Shangguan, W., Wei, N., Xin, Q., Yuan, H., Zhang, S., Liu, S., Lu, X., Wang, D., and Yan, F.: A review of the global soil property maps for Earth system models, SOIL, 5, 137–158, https://doi.org/10.5194/soil-5-137-2019, 2019a.

Dai, Y., Yuan, H., Xin, Q., Wang, D., Shangguan, W., Zhang, S., Liu, S., and Wei, N.: Different representations of canopy structure—A large source of uncertainty in global land surface modeling, Agricultural and Forest Meteorology, 269–270, 119–135, https://doi.org/10.1016/j.agrformet.2019.02.006, 2019b.

Dai, Y., Wei, N., Yuan, H., Zhang, S., Shangguan, W., Liu, S., Lu, X., and Xin, Y.: Evaluation of Soil Thermal Conductivity Schemes for Use in Land Surface Modeling, J Adv Model Earth Syst, 11, 3454–3473, https://doi.org/10.1029/2019MS001723, 2019c.

Dirmeyer, P. A.: The terrestrial segment of soil moisture-climate coupling, Geophys. Res. Lett., 38, L16702, https://doi.org/10.1029/2011GL048268, 2011.

Dy, C. Y. and Fung, J. C. H.: Updated global soil map for the Weather Research and Forecasting model and soil moisture initialization for the Noah land surface model, JGR Atmospheres, 121, 8777–8800, https://doi.org/10.1002/2015JD024558, 2016.

Entekhabi, D., Rodriguez-Iturbe, I., and Castelli, F.: Mutual interaction of soil moisture state and atmospheric processes, Journal of Hydrology, 184, 3–17, https://doi.org/10.1016/0022-1694(95)02965-6, 1996.

Essery, R.: Large-scale simulations of snow albedo masking by forests, Geophysical Research Letters, 40, 5521–5525, https://doi.org/10.1002/grl.51008, 2013.

Forzieri, G., Miralles, D. G., Ciais, P., Alkama, R., Ryu, Y., Duveiller, G., Zhang, K., Robertson, E., Kautz, M., Martens, B., Jiang, C., Arneth, A., Georgievski, G., Li, W., Ceccherini, G., Anthoni, P., Lawrence, P., Wiltshire, A., Pongratz, J., Piao, S., Sitch, S., Goll, D. S., Arora, V. K., Lienert, S., Lombardozzi, D., Kato, E., Nabel, J. E. M. S., Tian, H., Friedlingstein, P., and Cescatti, A.: Increased control of vegetation on global terrestrial energy fluxes, Nat. Clim. Chang., 10, 356–362, https://doi.org/10.1038/s41558-020-0717-0, 2020.

Harper, A. B., Williams, K. E., McGuire, P. C., Duran Rojas, M. C., Hemming, D., Verhoef, A., Huntingford, C., Rowland, L., Marthews, T., Breder Eller, C., Mathison, C., Nobrega, R. L. B., Gedney, N., Vidale, P. L., Otu-Larbi, F., Pandey, D., Garrigues, S., Wright, A., Slevin, D., De Kauwe, M. G., Blyth, E., Ardö, J., Black, A., Bonal, D., Buchmann, N., Burban, B., Fuchs, K., de Grandcourt, A., Mammarella, I., Merbold, L., Montagnani, L., Nouvellon, Y., Restrepo-Coupe, N., and Wohlfahrt, G.: Improvement of modeling plant responses to low soil moisture in JULESvn4.9 and evaluation against flux tower measurements, Geosci. Model Dev., 14, 3269–3294, https://doi.org/10.5194/gmd-14-3269-2021, 2021.

Harper, K. L., Lamarche, C., Hartley, A., Peylin, P., Ottlé, C., Bastrikov, V., San Martín, R., Bohnenstengel, S. I., Kirches, G., Boettcher, M., Shevchuk, R., Brockmann, C., and Defourny, P.: A 29-year time series of annual 300 m resolution plant-functional-type maps for climate models, Earth Syst. Sci. Data, 15, 1465–1499, https://doi.org/10.5194/essd-15-1465-2023, 2023.

Humphrey, V., Berg, A., Ciais, P., Gentine, P., Jung, M., Reichstein, M., Seneviratne, S. I., and Frankenberg, C.: Soil moisture–atmosphere feedback dominates land carbon uptake variability, Nature, 592, 65–69, https://doi.org/10.1038/s41586-021-03325-5, 2021.

Launiainen, S., Katul, G. G., Kolari, P., Lindroth, A., Lohila, A., Aurela, M., Varlagin, A., Grelle, A., and Vesala, T.: Do the energy fluxes and surface conductance of boreal coniferous forests in Europe scale with leaf area?, Glob Change Biol, 22, 4096–4113, https://doi.org/10.1111/gcb.13497, 2016.

Li, J., Chen, F., Zhang, G., Barlage, M., Gan, Y., Xin, Y., and Wang, C.: Impacts of land cover and soil texture uncertainty on land model simulations over the central Tibetan Plateau, J. Adv. Model. Earth Syst., 10, 2121–2146, https://doi.org/10.1029/2018MS001377, 2018.

Li, J., Zhang, G., Chen, F., Peng, X., and Gan, Y.: Evaluation of land surface subprocesses and their impacts on model performance with global flux data, J. Adv. Model. Earth Syst., 11, 1329–1348, https://doi.org/10.1029/2018MS001606, 2019.

Lin, W., Yuan, H., Dong, W., Zhang, S., Liu, S., Wei, N., Lu, X., Wei, Z., Hu, Y., and Dai, Y.: Reprocessed MODIS Version 6.1 Leaf Area Index Dataset and Its Evaluation for Land Surface and Climate Modeling, Remote Sensing, 15, 1780, https://doi.org/10.3390/rs15071780, 2023.

Mariotti, A., Ruti, P. M., and Rixen, M.: Progress in subseasonal to seasonal prediction through a joint weather and climate community effort, npj Clim Atmos Sci, 1, 4, https://doi.org/10.1038/s41612-018-0014-z, 2018.

Melton, J. R., Arora, V. K., Wisernig-Cojoc, E., Seiler, C., Fortier, M., Chan, E., and Teckentrup, L.: CLASSIC v1.0: the open-source community successor to the Canadian Land Surface Scheme (CLASS) and the Canadian Terrestrial Ecosystem Model (CTEM) – Part 1: Model framework and site-level performance, Geosci. Model Dev., 13, 2825–2850, https://doi.org/10.5194/gmd-13-2825-2020, 2020.

Ménard, C. B., Ikonen, J., Rautiainen, K., Aurela, M., Arslan, A. N., and Pulliainen, J.: Effects of Meteorological and Ancillary Data, Temporal Averaging, and Evaluation Methods on Model Performance and Uncertainty in a Land Surface Model, Journal of Hydrometeorology, 16, 2559–2576, https://doi.org/10.1175/JHM-D-15-0013.1, 2015.

Minasny, B. and McBratney, A. B.: Estimating the Water Retention Shape Parameter from Sand and Clay Content, Soil Sci. Soc. Am. J., 71, 1105–1110, https://doi.org/10.2136/sssaj2006.0298N, 2007.

Pastorello, G., Trotta, C., and Canfora, E.: The FLUXNET2015 dataset and the ONEFlux processing pipeline for eddy covariance data, Scientific Data, 7, 225, https://doi.org/10.1038/s41597-021-00851-9, 2020.

Pitman, A. J.: The evolution of, and revolution in, land surface schemes designed for climate models, Int. J. Climatol., 23, 479–510, https://doi.org/10.1002/joc.893, 2003.

Poulter, B., Ciais, P., Hodson, E., Lischke, H., Maignan, F., Plummer, S., and Zimmermann, N. E.: Plant functional type mapping for earth system models, Geosci. Model Dev., 4, 993–1010, https://doi.org/10.5194/gmd-4-993-2011, 2011.

Purdy, A. J., Fisher, J. B., Goulden, M. L., and Famiglietti, J. S.: Ground heat flux: An analytical review of 6 models evaluated at 88 sites and globally, J. Geophys. Res. Biogeosci., 121, 3045–3059, https://doi.org/10.1002/2016JG003591, 2016.

Shangguan, W., Dai, Y., Duan, Q., Liu, B., and Yuan, H.: A global soil data set for earth system modeling, J. Adv. Model. Earth Syst., 6, 249–263, https://doi.org/10.1002/2013MS000293, 2014.

Shi, J., & Yuan, H., Lin, W., & Dong, W.: A flux tower site attribute dataset intended for land surface modeling [Data set]. Zenodo. https://doi.org/10.5281/zenodo.10939725.

Stevens, D., Miranda, P. M. A., Orth, R., Boussetta, S., Balsamo, G., and Dutra, E.: Sensitivity of Surface Fluxes in the ECMWF Land Surface Model to the Remotely Sensed Leaf Area Index and Root Distribution: Evaluation with Tower Flux Data, Atmosphere, 11, 1362, https://doi.org/10.3390/atmos11121362, 2020.

Still, C. J., Berry, J. A., Collatz, G. J., and DeFries, R. S.: Global distribution of C_3 and C_4 vegetation: Carbon cycle implications, Global Biogeochem. Cycles, 17, 6-1-6–14, https://doi.org/10.1029/2001GB001807, 2003.

Stockli, R., Lawrence, D. M., Bonan, G. B., Denning, A. S., and Running, S. W.: Use of FLUXNET in the Community Land Model development, J. Geophys. Res., 113, 19, https://doi.org/10.1029/2007JG000562, 2008.

Swenson, S. C., Burns, S. P., and Lawrence, D. M.: The Impact of Biomass Heat Storage on the Canopy Energy Balance and Atmospheric Stability in the Community Land Model, J Adv Model Earth Syst, 11, 83–98, https://doi.org/10.1029/2018MS001476, 2019.

Ukkola, A. M., De Kauwe, M. G., Pitman, A. J., Best, M. J., Abramowitz, G., Haverd, V., Decker, M., and Haughton, N.: Land surface models systematically overestimate the intensity, duration and magnitude of seasonal-scale evaporative droughts, Environ. Res. Lett., 11, 104012, https://doi.org/10.1088/1748-9326/11/10/104012, 2016a.

Ukkola, A. M., Pitman, A. J., Decker, M., De Kauwe, M. G., Abramowitz, G., Kala, J., and Wang, Y.-P.: Modelling evapotranspiration during precipitation deficits: identifying critical processes in a land surface model, Hydrol. Earth Syst. Sci., 20, 2403–2419, https://doi.org/10.5194/hess-20-2403-2016, 2016b.

Ukkola, A. M., Haughton, N., De Kauwe, M. G., Abramowitz, G., and Pitman, A. J.: FluxnetLSM R package (v1.0): a community tool for processing FLUXNET data for use in land surface modelling, Geosci. Model Dev., 10, 3379–3390, https://doi.org/10.5194/gmd-10-3379-2017, 2017.

Ukkola, A. M., Abramowitz, G., and De Kauwe, M. G.: A flux tower dataset tailored for land model evaluation, Earth Syst. Sci. Data, 14, 449–461, https://doi.org/10.5194/essd-14-449-2022, 2022.

Williams, I. N. and Torn, M. S.: Vegetation controls on surface heat flux partitioning, and land-atmosphere coupling, Geophysical Research Letters, 42, 9416–9424, https://doi.org/10.1002/2015GL066305, 2015.

Williams, M., Richardson, A. D., Reichstein, M., Stoy, P. C., Peylin, P., Verbeeck, H., Carvalhais, N., Jung, M., Hollinger, D. Y., Kattge, J., Leuning, R., Luo, Y., Tomelleri, E., and Trudinger, C. M.: Improving land surface models with FLUXNET data, Biogeosciences, 6, 1341–1359, https://doi.org/10.5194/bg-6-1341-2009, 2009.

Wilson, K., Goldstein, A., Falge, E., Aubinet, M., Baldocchi, D., Berbigier, P., Bernhofer, C., Ceulemans, R., Dolman, H., Field, C., Grelle, A., Ibrom, A., Law, B. E., Kowalski, A., Meyers, T., Moncrieff, J., Monson, R., Oechel, W., Tenhunen, J., Valentini, R., and Verma, S.: Energy balance closure at FLUXNET sites, Agricultural and Forest Meteorology, 113, 223–243, https://doi.org/10.1016/S0168-1923(02)00109-0, 2002.

Zhang, X., Dai, Y., Cui, H., Dickinson, R. E., Zhu, S., Wei, N., Yan, B., Yuan, H., Shangguan, W., Wang, L., and Fu, W.: Evaluating common land model energy fluxes using FLUXNET data, Adv. Atmos. Sci., 34, 1035–1046, https://doi.org/10.1007/s00376-017-6251-y, 2017.

Zhu, S., Chen, H., Zhang, X., Wei, N., Shangguan, W., Yuan, H., Zhang, S., Wang, L., Zhou, L., and Dai, Y.: Incorporating root hydraulic redistribution and compensatory water uptake in the Common Land Model: Effects on site level and global land modeling, J. Geophys. Res. Atmos., 122, 7308–7322, https://doi.org/10.1002/2016JD025744, 2017.